The pre-inflationary and inflationary fast-roll eras and their signatures in the low CMB multipoles

C. Destri [(a)],* **H. J. de Vega** [(b,c)],† **and N. G. Sanchez** [(c)]‡

[(a)] *Dipartimento di Fisica G. Occhialini, Università Milano-Bicocca and INFN, sezione di Milano-Bicocca, Piazza della Scienza 3, 20126 Milano, Italia.*

[(b)] *LPTHE, Université Pierre et Marie Curie (Paris VI) et Denis Diderot (Paris VII), Laboratoire Associé au CNRS UMR 7589, Tour 24, 5ème. étage, Boite 126, 4, Place Jussieu, 75252 Paris, Cedex 05, France.*

[(c)] *Observatoire de Paris, LERMA. Laboratoire Associé au CNRS UMR 8112. 61, Avenue de l'Observatoire, 75014 Paris, France.*

(Dated: February 15, 2010)

We study the entire coupled evolution of the inflaton $\phi(t)$ and the scale factor $a(t)$ for general initial conditions $\phi(t_0)$ and $d\phi(t_0)/dt$ at a given initial time t_0. The **generic** early universe evolution has three stages: decelerated fast-roll followed by inflationary fast-roll and then inflationary slow-roll (an attractor always reached for **generic** initial conditions). This evolution is valid for all regular inflaton potentials $v(\phi)$. In addition, we find a special (extreme) slow-roll solution starting at $t = -\infty$ in which the fast-roll stages are absent. At some time $t = t_*$, the evolution backwards in time from t_0 reaches generically a mathematical singularity where $a(t)$ vanishes and the Hubble parameter becomes singular. We determine the general behaviour near the singularity. The classical homogeneous inflaton description turns to be valid for $t - t_* > 10\, t_{Planck}$ well before the beginning of inflation, quantum loop effects are negligible there. The singularity is never reached in the validity region of the classical treatment and therefore it **is not a real physical phenomenon** here. Fast-roll and slow-roll regimes are analyzed in detail including the equation of state evolution, both analytically and numerically. The characteristic time scale of the fast-roll era turns to be $t_1 = (1/m)\, \sqrt{V(0)/[3\, M^4]} \sim 10^4\, t_{Planck}$ where V is the double-well inflaton potential, m is the inflaton mass and M the energy scale of inflation. The **whole** evolution of the fluctuations along the decelerated and inflationary fast-roll and slow-roll eras is computed. The Bunch-Davies initial conditions (BDic) are generalized for the present case in which the potential felt by the fluctuations can never be neglected. The fluctuations feel a **singular attractive** potential near the $t = t_*$ singularity (as in the case of a particle in a central singular potential) with **exactly** the **critical** strength $(-1/4)$ allowing the fall to the centre. Precisely, the fluctuations exhibit logarithmic behaviour describing the fall to $t = t_*$. The power spectrum gets dynamically modified by the effect of the fast-roll eras and the choice of BDic at a finite time through the transfer function $D(k)$ of initial conditions. The power spectrum vanishes at $k = 0$. $D(k)$ presents a first peak for $k \sim 2/\eta_0$ (η_0 being the conformal initial time), then oscillates with decreasing amplitude and vanishes asymptotically for $k \to \infty$. The transfer function $D(k)$ affects the **low** CMB multipoles C_ℓ: the change $\Delta C_\ell/C_\ell$ for $1 \leq \ell \leq 5$ is computed as a function of the starting instant of the fluctuations t_0. CMB quadrupole observations indicate large **suppressions** which are well reproduced for the range $t_0 - t_* \gtrsim 0.05/m \simeq 10100\, t_{Planck}$.

Contents

*Electronic address: Claudio.Destri@mib.infn.it
†Electronic address: devega@lpthe.jussieu.fr
‡Electronic address: Norma.Sanchez@obspm.fr

I. INTRODUCTION AND SUMMARY OF RESULTS

Since the Universe expands exponentially fast during inflation, gradients are exponentially erased and can be neglected. At the same time, the exponential stretching of spatial lengths **classicalizes** the physics and allows a **classical** treatment. One can therefore consider a homogeneous and classical inflaton field which thus determines self-consistently a homogenous and isotropic Friedman-Robertson Walker metric sourced by this inflaton.

This treatment is valid for early times well after the Planck time $t = 10^{-44}$ sec., at which the quantum fluctuations are expected to be large and thus a full quantum gravity treatment is required.

In this paper we study the entire coupled evolution of the inflaton field $\phi(t)$ and the scale factor $a(t)$ of the metric for generic initial conditions, fixed by the values of $\phi(t_0)$ and $d\phi(t_0)/dt$ at a given initial time t_0.

We show that the **generic** early universe evolution has three stages: a decelerated fast-roll stage followed by an inflationary fast-roll stage and then by a slow-roll inflationary regime which is an attractor always reached for **generic** initial conditions. This evolution is valid for all regular inflaton potentials. In addition, we find a particular (extreme) slow-roll solution starting from $t = -\infty$ in which the fast-roll stages are absent.

The evolution backwards in time from t_0 reachs generically a mathematical singularity at some time $t = t_*$ where the scale factor $a(t)$ vanishes, and the Hubble parameter becomes singular.

We find the general behaviour of the inflaton and the scale factor near the singularity as given by eqs. (2.14)-(2.17) and determine the validity of the classical approximation, namely $(H/M_{Pl})^2 \ll 1$. It must be stressed that such mathematical singularity is attained extrapolating the classical treatment where it is **no more valid**. The singularity is never reached in the validity region of the classical treatment and therefore such mathematical singularity **is not a real physical phenomenon** here.

Quantum loops effects turns to be less than 1% for $t - t_* > 10^{-42}$ sec and therefore the classical treatment of the inflaton and the space-time can be trusted well before the begining of inflation.

The fast-roll (both decelerated and inflationary) and slow-roll regimes are analyzed in detail, with both the exact numerical evolution and an analytic approximation, and the whole equation of state evolution in the three regimes. We consider here the double well (broken symmetric) fourth order inflaton potential since it gives the best description of the CMB+LSS data [2, 7] within the Ginsburg-Landau effective theory approach we follow.

The characteristic time scale of the fast-roll era turns to be $t_1 = (1/m)\ \sqrt{V(0)/[3\ M^4]} \sim 10^4\ t_{Planck}$ where $V(0)$ is the double well inflaton potential at zero inflaton field, m is the inflaton mass and M the energy scale of inflation. The time scale of the inflaton in the extreme slow roll solution goes as the inverse of t_1, namely $1/[m^2\ t_1]$.

We study the **whole** evolution of the curvature and tensor fluctuations along the three succesive regimes: decelerated fast-roll followed by inflationary fast-roll and then inflationary slow-roll, and compute the power spectrum by the end of inflation. The fluctuations feel a **singular attractive** potential near the $t = t_*$ singularity (as in the case of a particle in a central singular potential) with **exactly** the **critical** strength $(-1/4)$ for which the fall to the centre

becomes possible. Precisely, the logarithmic behaviour of the fluctuations for $t \to t_*$ eq.(4.3) describes the fall to $t = t_*$ for the critical strength of the potential $W_{\mathcal{R}}$ felt by the fluctuations.

We generalize the Bunch-Davies initial conditions (BDic) to the present case in which the potential felt by the fluctuations can never be neglected.

In general, the mode functions for large k behave as free modes since the potential $W_{\mathcal{R}}$ becomes negligible in this limit except at the singularity $t = t_*$. One can then impose Bunch-Davies conditions for large k which corresponds to assume an initial quantum vacuum Fock state, empty of curvature excitations

$$S_{\mathcal{R}}(k;\eta) \stackrel{k\to\infty}{=} \frac{e^{-i\,k\,\eta}}{\sqrt{2\,k}} \tag{1.1}$$

and therefore

$$\frac{dS_{\mathcal{R}}}{d\eta}(k;\eta_0) \stackrel{k\to\infty}{=} -i\,k\,S_{\mathcal{R}}(k;\eta_0)\ .$$

Here η stands for the conformal time: $d\eta = dt/a(t)$. Eq.(1.1) fulfils the Wronskian normalization (that ensures the canonical commutation relations)

$$W[S_{\mathcal{R}}, S^*_{\mathcal{R}}] = S_{\mathcal{R}}\,\frac{dS^*_{\mathcal{R}}}{d\eta} - \frac{dS_{\mathcal{R}}}{d\eta}\,S^*_{\mathcal{R}} = i\ . \tag{1.2}$$

In asymptotically flat (or conformally flat) regions of the space-time the potential felt by the fluctuations $W_{\mathcal{R}}(\eta)$ vanishes and the fluctuations exhibit a plane wave behaviour for **all** k (not necesarily large). This is not the case in strong gravity fields or near curvature singularities as in the present cosmological space-time where $W_{\mathcal{R}}(\eta)$ can never be neglected at fixed k. However, we can choose Bunch-Davies initial conditions (BDic) at $\eta = \eta_0$ (or equivalently, $t = t_0$) by imposing

$$\frac{dS_{\mathcal{R}}}{d\eta}(k;\eta_0) = -i\,k\,S_{\mathcal{R}}(k;\eta_0) \quad \text{for all } k\ . \tag{1.3}$$

That is, we consider the initial value problem for the mode functions giving the values of $S_{\mathcal{R}}(k;\eta)$ and $dS_{\mathcal{R}}/d\eta$ at $\eta = \eta_0$. This condition combined with the Wronskian condition eq.(1.2) implies that

$$|S_{\mathcal{R}}(k;\eta_0)| = \frac{1}{\sqrt{2\,k}} \quad , \quad \left|\frac{dS_{\mathcal{R}}}{d\eta}(k;\eta_0)\right| = \sqrt{\frac{k}{2}}\ . \tag{1.4}$$

which is equivalent to eq.(1.1) for large k.

The power spectrum at the end of slow-roll inflation $P_{\mathcal{R}}(k)$ gets dynamically modified by the effect of the preceding fast-roll eras through the transfer function of initial conditions $D(k)$:

$$P_{\mathcal{R}}(k) = P^{BD}_{\mathcal{R}}(k)\,[1 + D(k)]\ , \tag{1.5}$$

$D(k)$ accounts for the effect of both the initial conditions and the fluctuations evolution during fast-roll (before slow-roll). $D(k)$ depends on the time t_0 at which BDic are imposed.

The power spectrum $P^{BD}_{\mathcal{R}}(k)$ corresponds to start the evolution with pure slow-roll from $t_0 \to -\infty$ and with BDic eq.(1.3)-eq.(1.4) imposed there at $t_0 \to -\infty$, that is $\eta_0 = -\infty$. $P^{BD}_{\mathcal{R}}(k)$ is given by its customary pure slow-roll expression,

$$\log P^{BD}_{\mathcal{R}}(k) = \log A_s(k_0) + (n_s - 1)\,\log\frac{k}{k_0} + \tfrac{1}{2}\,n_{run}\,\log^2\frac{k}{k_0} + \mathcal{O}\left(\frac{1}{N^3}\right)\ . \tag{1.6}$$

where N is the number of inflation efolds since the pivot CMB scale k_0 exits the horizon. We take here $N = 60$.

Actually, BDic can be imposed at $\eta = \eta_0 = -\infty$ if and only if the inflaton evolution **also** starts at $\eta = \eta_0 = -\infty$. This **only** happens for a *particular* inflaton solution: the *extreme slow-roll* solution that we explicitly present and analyze in sec. III A. In the extreme slow–roll case the fast-roll eras are absent, BDic are imposed at $t_0 \to -\infty$ (that is $\eta_0 = -\infty$), then $D(k) = 0$ and $P_{\mathcal{R}}(k) = P^{BD}_{\mathcal{R}}(k)$. Only in this case the fluctuation power spectrum at the end of inflation is the usual power spectrum $P^{BD}_{\mathcal{R}}(k)$ eq.(4.24).

When BDic are imposed at **finite times** t_0, the spectrum **is not** the usual $P_{\mathcal{R}}^{BD}(k)$ but it gets modified by a non-zero transfer function $D(k)$ eq.(4.21). The power spectrum $P_{\mathcal{R}}(k)$ vanishes at $k = 0$ and exhibits oscillations which vanish at large k [see figs. 6 and 7]

Generically, the power spectrum vanishes at $k = 0$ and we thus have

$$1 + D(k) \stackrel{k\to 0}{=} \mathcal{O}(k^{n_s+1}) \quad . \tag{1.7}$$

as shown in sec. V A. $D(k)$ presents a first peak for $k \sim 2/\eta_0$ and then oscillates asymptotically with decreasing amplitude such that

$$D(k) \stackrel{k\to\infty}{=} \mathcal{O}\left(\frac{1}{k^2}\right) . \tag{1.8}$$

We solved numerically the fluctuations equation with the BDic eq.(4.7) covering both the fast-roll and slow-roll regimes, namely for different initial times t_0 ranging from the singularity $\tau = \tau_*$ till the transition time τ_{trans} from fast-roll to slow-roll. That is to say, we solved the fluctuations evolution for BDic imposed at different times in the three eras and we compare the resulting power spectra among them. We computed the corresponding transfer function, $D(k)$ for the BDic imposed at the different eras. We depict $1 + D(k)$ vs. k for the different values of the time t_0 where BDic are imposed in figs. 6.

When the BDic are imposed during the fast–roll stage well **before** it ends, $D(k)$ changes much more significantly than along the extreme slow roll solution. This is due to two main effects: the potential felt by the fluctuations is attractive during fast–roll, and η_0, (far from being almost proportional to $1/a(\eta)$), tends to the constant value η_* as $\tau \to \tau_*^+$ and $a(\eta) \to 0$. The numerical transfer functions $1 + D(k)$ obtained from eqs.(4.12) and (4.21) are plotted in figs. 6.

We have also computed $D(k)$ analytically with BDic at finite times η_0, and a simple form is obtained in the scale invariant case, which is the leading term in the slow-roll expansion:

$$D(k) = \frac{\cos 2x}{x^2} - \frac{\sin 2x}{x^3} + \frac{\sin^2 x}{x^4} \quad , \quad x \equiv k\,\eta_0 \, . \tag{1.9}$$

Different initial times t_0 lead essentially to a rescaling of k in $D(k)$ by a factor η_0 since the conformal time η is almost proportional to $1/a(\eta)$ during slow-roll [see figs. 6 and below eq.(5.7)]. By virtue of the dynamical attractor character of slow–roll, the power spectrum when the BDic are imposed at a finite time t_0 cannot really distinguish between the extreme slow–roll solution or any other solution which is attracted to slow–roll well before the time t_0.

Using the transfer function $D(k)$ we obtained, we computed the change on the CMB multipoles $\Delta C_\ell/C_\ell$ for $\ell = 1, 2$ and 3 as functions of the starting instant of the fluctuations t_0. We plot $\Delta C_\ell/C_\ell$ for $1 \leq \ell \leq 5$ vs. $t_0 - t_*$ in fig. 9. We see that $\Delta C_\ell/C_\ell$ is **positive** for small $t_0 - t_*$ and **decreases** with t_0 becoming then **negative**. The CMB quadrupole observations indicate a large **suppression** thus indicating that $t_0 - t_* \gtrsim 0.05/m \simeq 10100\, t_{Planck}$.

The fact that choosing BDic leads to a primordial power and its respective CMB multipoles which correctly **reproduce** the observed spectrum justifies the use of BDic.

Besides finding a CMB quadrupole suppression in agreement with observations [2]-[6], we provide here **predictions** for the dipole and $\ell \leq 5$-multipole suppressions. Forthcoming CMB observations can provide better data to confront our CMB multipole suppression predictions. It will be extremely interesting to measure the primordial dipole and compare with our predicted value.

II. THE PRE-INFLATIONARY AND INFLATIONARY FAST-ROLL ERAS

The current WMAP data are validating the single field slow-roll scenario [1]. Single field slow-roll models provide an appealing, simple and fairly generic description of inflation. This inflationary scenario can be implemented using a scalar field, the *inflaton* with a Lagrangian density (see for example ref. [2])

$$\mathcal{L} = a^3(t)\left[\frac{\dot\varphi^2}{2} - \frac{(\nabla\varphi)^2}{2\,a^2(t)} - V(\varphi)\right] , \tag{2.1}$$

where $V(\varphi)$ is the inflaton potential. Since the universe expands exponentially fast during inflation, gradient terms are exponentially suppressed and can be neglected. At the same time, the exponential stretching of spatial lengths classicalize the physics and permits a classical treatment. One can therefore consider an homogeneous and classical inflaton field $\varphi(t)$ which obeys the evolution equation

$$\ddot{\varphi} + 3\,H(t)\,\dot{\varphi} + V'(\varphi) = 0 \tag{2.2}$$

in the isotropic and homogeneous FRW metric which is sourced by the inflaton

$$ds^2 = dt^2 - a^2(t)\,d\vec{x}^2 \tag{2.3}$$

$H(t) \equiv \dot{a}(t)/a(t)$ stands for the Hubble parameter. The energy density and the pressure for a spatially homogeneous inflaton are given by

$$\rho = \frac{\dot{\varphi}^2}{2} + V(\varphi) \quad , \quad p = \frac{\dot{\varphi}^2}{2} - V(\varphi)\ . \tag{2.4}$$

Threfore, the scale factor $a(t)$ obeys the Friedmann equation,

$$H^2(t) = \frac{1}{3M_{Pl}^2}\left[\frac{1}{2}\,\dot{\varphi}^2 + V(\varphi)\right]\ . \tag{2.5}$$

In order to have a finite number of inflation efolds, the inflaton potential $V(\varphi)$ must vanish at its absolute minimum

$$V'(\varphi_{min}) = V(\varphi_{min}) = 0 \tag{2.6}$$

Otherwise, inflation continues forever.

We formulate inflation as an effective field theory within the Ginsburg-Landau spirit [2, 10, 17]. The theory of the second order phase transitions, the Ginsburg-Landau theory of superconductivity, the current-current Fermi theory of weak interactions, the sigma model of pions, nucleons (as skyrmions) and photons are all successful effective field theories. Our work shows how powerful is the effective theory of inflation **to predict observable quantities** that can be or will be soon contrasted with experiments.

The effective theory of inflation should be the low energy limit of a microscopic fundamental theory not yet precisely known. The energy scale of inflation M should be at the Grand Unified Theory (GUT) energy scale in order to reproduce the amplitude of the CMB anisotropies [2]. Therefore, the microscopic theory of inflation is expected to be a GUT in a cosmological space-time. Such a theory of inflation would contain many fields of various spins. However, in order to have a homogeneous and isotropic universe the expectation value of the energy-momentum tensor of the fields must be homogeneous and isotropic. The inflaton field in the effective theory may be a coarse-grained average of fundamental scalar fields, or a composite (bound state) of fundamental fields of higher spin, just as in superconductivity. The inflaton does not need to be a fundamental field, for example it may emerge as a condensate of fermion-antifermion pairs $< \bar{\Psi}\Psi >$ in a GUT in the cosmological background. In order to describe the cosmological evolution is enough to consider the effective dynamics of such condensates. The relation between the effective field theory of inflation and the microscopic fundamental GUT is akin to the relation between the effective Ginzburg-Landau theory of superconductivity and the microscopic BCS theory, or like the relation of the $O(4)$ sigma model, an effective low energy theory of pions, photons and chiral condensates with quantum chromodynamics (QCD) [16].

Vector fields have been considered to describe inflation in ref.[14]. The results for the inflaton should not be very different from the effective inflaton description since the energy-momentum tensor of the vector field is to be taken homogeneous and isotropic. Namely, we are always in the presence of a scalar condensate.

Since the mass of the inflaton is given by $M^2/M_{Pl} \sim 10^{13}$GeV [2], massless fields alone cannot describe inflation which leads to the observed amplitude of the CMB anisotropies.

The classical inflaton potential $V(\varphi)$ gets modified by quantum loop corrections. We computed relevant quantum loop corrections to inflationary dynamics in ref. [2, 15]. A thorough study of the effect of quantum fluctuations reveals that these loop corrections are suppressed by powers of $(H/M_{Pl})^2 \sim 10^{-9}$ where H is the Hubble parameter during inflation [2, 15]. Therefore, quantum loop corrections are very small, a conclusion that validates the reliability of the classical approximation and of the effective field theory approach to inflationary dynamics. In particular, the (small) one-loop corrections to the potential in an inflationary universe are very different from the Coleman-Weinberg form [2, 15].

We choose the inflaton field initially homogeneous which ensures it is always homogeneous. The fluctuations around are small and give small corrections to the homogeneity of the Universe. The rapid expansion of the Universe, in the inflationary regimes, takes care of the classical fluctuations, quickly flattening an eventually non-homogeneous condensate.

A. The complete inflaton evolution through the different eras

It is convenient to use the dimensionless variables to analyze the inflaton evolution equations eqs.(2.2)-(2.5), [2]:

$$\tau = m\, t \quad , \quad h \equiv \frac{H}{m} \quad , \quad \phi = \frac{\varphi}{M_{Pl}} \; . \tag{2.7}$$

The inflaton potential has then the universal form

$$V(\varphi) = M^4 \, v\left(\frac{\varphi}{M_{Pl}}\right) \; , \tag{2.8}$$

where M is the energy scale of inflation and $v(\phi)$ is a dimensionless function. Without loss of generality we can set $v'(0) = 0$ [2]. Moreover, provided $V''(0) \neq 0$ we can set without loss of generality $|v''(0)| = 1/2$. Namely, we have for small fields,

$$v(\phi) \stackrel{\phi \to 0}{=} v(0) \mp \frac{1}{2}\, \phi^2 + \mathcal{O}(\phi^3) \tag{2.9}$$

where the minus sign in the quadratic term corresponds to new inflation and the plus sign to chaotic inflation.

In these dimensionless variables, the energy density and the pressure for a spatially homogeneous inflaton are given from eq.(2.4) by

$$\frac{\rho}{M^4} = \frac{1}{2}\left(\frac{d\phi}{d\tau}\right)^2 + v(\phi) \quad , \quad \frac{p}{M^4} = \frac{1}{2}\left(\frac{d\phi}{d\tau}\right)^2 - v(\phi) \; , \tag{2.10}$$

and the coupled inflaton evolution equation (2.2) and the Friedmann equation (2.5) take the form [2],

$$\begin{aligned} &\frac{d^2\phi}{d\tau^2} + 3\, h\, \frac{d\phi}{d\tau} + v'(\phi) = 0 \quad , \\ &h^2(\tau) = \frac{1}{3}\left[\frac{1}{2}\left(\frac{d\phi}{d\tau}\right)^2 + v(\phi)\right] \quad . \end{aligned} \tag{2.11}$$

These coupled nonlinear differential equations completely define the time evolution of the inflaton field and the scale factor once the initial conditions are given at the initial time τ_0. Namely, the initial conditions are fixed by giving two real numbers, the values of $\phi(\tau_0)$ and $d\phi(\tau_0)/d\tau$.

It follows from eqs.(2.11) that

$$\frac{d^2 a}{d\tau^2} = \frac{1}{3}\left[v(\phi) - \left(\frac{d\phi}{d\tau}\right)^2\right] = -\frac{1}{2}\left(p + \frac{1}{3}\,\rho\right) \; . \tag{2.12}$$

When $d^2a/d\tau^2 > 0$ the expansion of the universe accelerates and it is then called inflationary.

The derivative of the Hubble parameter is **always** negative:

$$\frac{dh}{d\tau} = -\frac{1}{2}\left(\frac{d\phi}{d\tau}\right)^2 \; . \tag{2.13}$$

Therefore $h(\tau)$ decreases monotonically with increasing τ. Conversely, if we evolve the solution backwards in time from τ_0, $h(\tau)$ will generically **increase** without bounds. Namely, at some time $\tau = \tau_*$, $h(\tau)$ can exhibit a singularity where simultaneously $a(\tau_*)$ vanishes.

In fact, the equations (2.11) admit the singular solution for $\tau \to \tau_*$,

$$\phi(\tau) \stackrel{\tau \to \tau_*}{=} \sqrt{\frac{2}{3}}\, \log\frac{\tau - \tau_*}{b} \to -\infty \quad , \quad h(\tau) \equiv \frac{d}{d\tau}\log a(\tau) \stackrel{\tau \to \tau_*}{=} \frac{1}{3\,(\tau - \tau_*)} \to +\infty \; , \tag{2.14}$$

where b is an integration constant. The energy density $\epsilon(\tau)$ and equation of state take the limiting form,

$$\rho(\tau) \stackrel{\tau \to \tau_*}{=} \frac{1}{3\,(\tau - \tau_*)^2} \to +\infty \quad , \quad \frac{p(\tau)}{\rho(\tau)} \stackrel{\tau \to \tau_*}{=} 1 \; . \tag{2.15}$$

Namely, the limiting equation of state is $p \stackrel{\tau\to\tau_*}{=} +\rho$.

We have in this regime

$$a(\tau) \stackrel{\tau\to\tau_*}{=} C\,(\tau-\tau_*)^{\frac{1}{3}} \to 0\,, \tag{2.16}$$

where C is some constant. That is, the geometry becomes singular for $\tau \to \tau_*$. The behaviour near τ_* is non-inflationary, namely decelerated, since

$$\frac{d^2a}{d\tau^2} \stackrel{\tau\to\tau_*}{=} -\frac{2}{9}\,(\tau-\tau_*)^{-\frac{5}{3}} \to -\infty\,. \tag{2.17}$$

For $\tau \to \tau_*$, near the singularity, the potential $v(\phi)$ becomes negligible in eqs.(2.11). Therefore, eqs.(2.14)-(2.17) are valid for all regular potentials $v(\phi)$.

The evolution starts thus by this decelerated fast-roll regime followed by an inflationary fast-roll regime and then by a slow-roll inflationary regime [2]. Recall that the slow-roll regime is an **attractor** [4], and therefore the inflaton always reaches a slow-roll inflationary regime for **generic** initial conditions. We display in fig. 1 the inflaton flow in phase space, namely $d\phi/d\tau$ vs. ϕ for different initial conditions.

The number of efolds of slow-roll inflation N_{sr} is determined by the time when the inflaton trajectory reaches the red quasi-horizontal line of slow-roll regime [see fig. 1]. We see that $d\phi/d\tau$ decreases steeply with ϕ. This implies that N_{sr} is mainly determined by the initial value of ϕ with a mild (logarithmic) dependence on the initial value of $d\phi/d\tau$

The inflaton flow described by eq.(2.14) results

$$\dot\phi(\tau) \stackrel{\tau\to\tau_*}{=} \sqrt{\frac{2}{3}}\,\frac{e^{-\sqrt{\frac{3}{2}}\,\phi(\tau)}}{b} \tag{2.18}$$

which well reproduce the almost vertical blue and green lines in fig. 1.

The inflationary regimes are characterized by the slow-roll parameters ϵ_v and η_v [2]

$$\epsilon_v = \frac{1}{2\,h^2}\,\left(\frac{d\phi}{d\tau}\right)^2 \quad , \quad \eta_v = \frac{v''(\phi)}{v(\phi)}\,. \tag{2.19}$$

The slow-roll behaviour is defined by the condition $\epsilon_v < 1/N$. Typically, $\epsilon_v \lesssim 1/N$ during slow-roll. More generally accelerated expansion (inflation) happens for $\epsilon_v < 1$ while we have decelerated expansion for $\epsilon_v > 1$ as follows from eqs.(2.10)-(2.12) and (2.19).

The parameter η_v is also of the order $1/N$ during slow-roll and it is generically of order $1/N$ during fast-roll except when the potential $v(\phi)$ vanishes.

Eq.(2.13) implies a monotonic decreasing of the expansion rate of the universe. There are **four stages** in the universe evolution described by eqs.(2.11):

- The non-inflationary fast-roll stage starting at the singularity $\tau = \tau_*$ and ending when $d^2a/d\tau^2$ becomes positive [see eq.(2.12)].
- The inflationary fast-roll stage starts when $d^2a/d\tau^2$ becomes positive and ends at $\tau = \tau_{trans}$ when ϵ_v becomes smaller than $1/N$ [see eq.(2.19)].
- The inflationary slow-roll stage follows, and it continues as long as $\epsilon_v < 1/N$ and $d^2a/d\tau^2 > 0$. It ends when $d^2a/d\tau^2$ becomes negative at $\tau = \tau_{end}$.
- A matter-dominated stage follows the inflationary era.

The four stages described above correspond to the evolution for generic initial conditions or, equivalently, starting from the singular behaviour eqs.(2.14). In addition, there exists a special (extreme) slow-roll solution starting at $\tau = -\infty$ where the fast-roll stages are absent. We derive this extreme slow-roll solution in sec. III A.

As shown in refs. [2, 7] the double well (broken symmetric) fourth order potential

$$V(\varphi) = \frac{1}{4}\,\lambda\,\left(\varphi^2 - \frac{m^2}{\lambda}\right)^2 = -\frac{1}{2}\,m^2\,\varphi^2 + \frac{1}{4}\,\lambda\,\varphi^4 + \frac{m^4}{4\,\lambda} \tag{2.20}$$

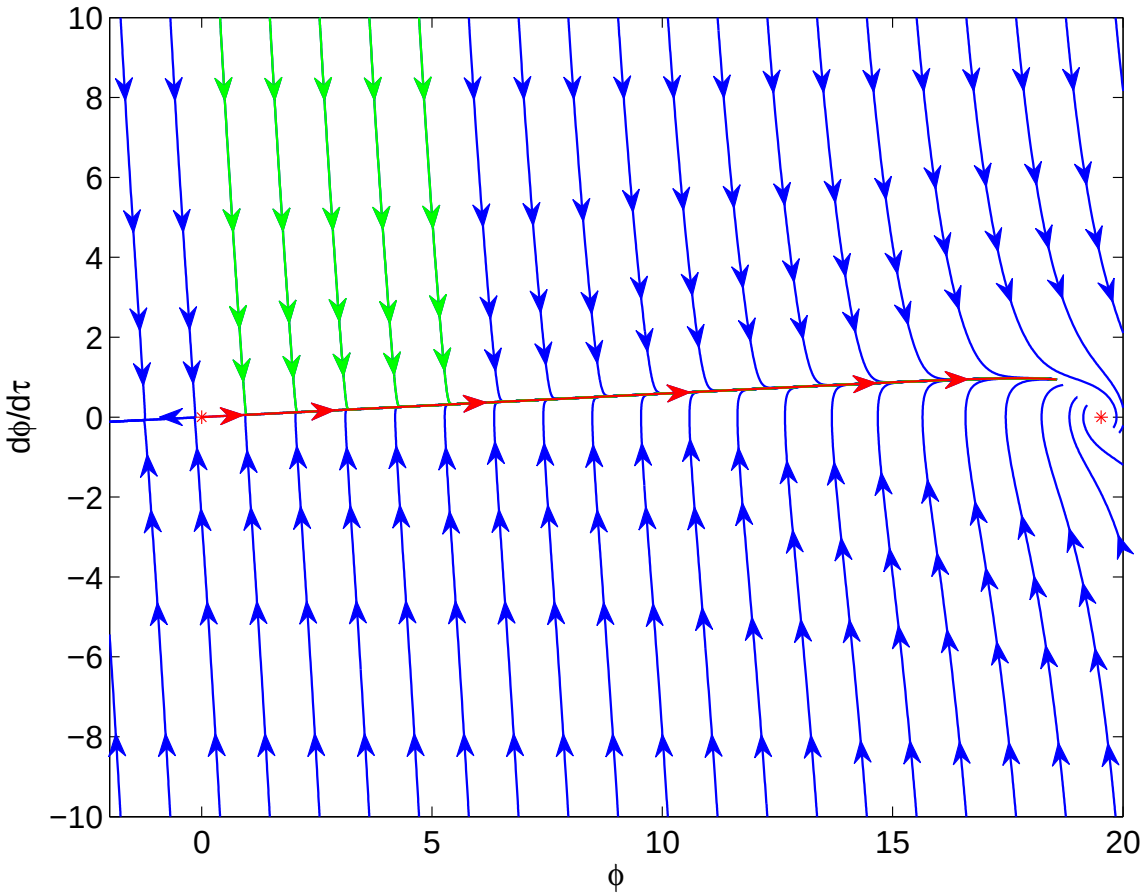

FIG. 1: The complete inflaton flow in phase space. $d\phi/d\tau$ vs. ϕ for different initial conditions. We see that the inflaton always reaches a slow-roll regime for generic initial conditions represented by a red quasi-horizontal line. Hence, the slow-roll line is an attractor. Ultimately the inflaton reaches asymptotically the absolute minima $d\phi/d\tau = 0,\ \phi = \phi_{min} = \sqrt{8\,N/y} = 19.52\ldots$. The number of efolds of slow-roll inflation N_{sr} increases for decreasing initial $\phi > 0$ when $d\phi/d\tau > 0$ initially. The $\phi > 0,\ d\phi/d\tau > 0$ trajectories corresponding to $N_{sr} > 63$ are colored in green.

provides a very good fit for the CMB+LSS data, while at the same time being particularly simple, natural and stable in the Ginsburg-Landau sense. This is a new inflation model with the inflaton rolling from the vicinity of the local maxima of $V(\varphi)$ at $\varphi = 0$ towards the absolute minimum $\varphi = m/\sqrt{\lambda}$.

The inflaton mass m and coupling λ are naturally expressed in terms of the **two** relevant energy scales in this problem: the energy scale of inflation M and the Planck mass $M_{Pl} = 2.43534\ 10^{18}$ GeV,

$$m = \frac{M^2}{M_{Pl}}\ , \quad \lambda = \frac{y}{8\,N}\ \left(\frac{M}{M_{Pl}}\right)^4\ . \tag{2.21}$$

Here $N \sim 60$ is the number of efolds since the cosmologically relevant modes exit the horizon till the end of inflation and $y \sim 1$ is the quartic coupling.

The MCMC analysis of the CMB+LSS data combined with the theoretical input above yields the value $y \simeq 1.26$ for the coupling [2, 7]. y turns to be **order one** consistent with the Ginsburg-Landau formulation of the theory of inflation [2].

This model of new inflation yields as most probable values: $n_s \simeq 0.964,\ r \simeq 0.051$ [2, 7]. This value for r is within reach of forthcoming CMB observations. For $y > 0.431946\ldots$ and in particular for the best fit value $y \simeq 1.26$, the inflaton field exits the horizon in the negative concavity region $V''(\varphi) < 0$ intrinsic to new inflation [2]. We find for the best fit [2, 7],

$$M = 0.543 \times 10^{16}\ \ \text{GeV for the scale of inflation and}\ \ \ m = 1.21 \times 10^{13}\ \ \text{GeV for the inflaton mass.} \tag{2.22}$$

We consider from now on the quartic broken symmetric potential eq. (2.20) which becomes using eq.(2.8)]

$$v(\phi) = \frac{g}{4}\left(\phi^2 - \frac{1}{g}\right)^2 = -\frac{1}{2}\,\phi^2 + \frac{g}{4}\,\phi^4 + \frac{1}{4\,g} \quad \text{where} \quad g = \frac{y}{8\,N}\,. \tag{2.23}$$

We have two arbitrary real coefficients characterizing the initial conditions. We can choose them as b and τ_* [see eq.(2.14)]. A total number of slow-roll inflation efolds $N_{sr} \simeq 63$ permits to explain the CMB quadrupole suppression [2, 5, 6]. Such requirement fixes the value of b for a given coupling y.

We integrated numerically eqs.(2.11) with eq.(2.14) as initial conditions. We find that $b = 4.745272\ldots\ 10^{-5}$ yields 63 efolds of inflation during the slow-roll era for $y = 1.26$, the best fit to the CMB and LSS data. We find that b is a monotonically increasing function of the coupling y for fixed number of slow-roll efolds. At fixed coupling, b increases with the number of slow-roll efolds.

We display in fig. 2 b as a function of y and the number of slow–roll inflation efolds N_{sr}.

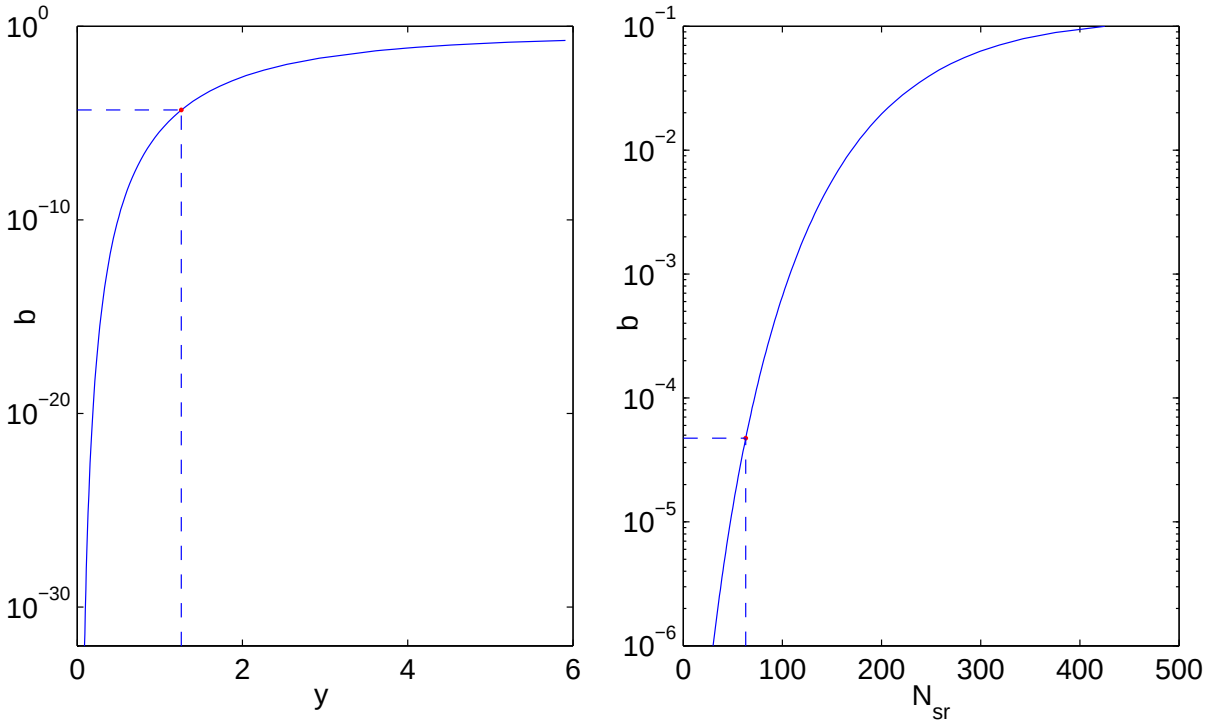

FIG. 2: Left panel: the coefficient b characterizing the initial conditions vs. the quartic coupling y for $N_{sr} = 63$ efolds of slow-roll inflation. Right panel: b vs. N_{sr} for $y = 1.26$. The preferred values $y = 1.26$ and N_{sr} are highlighted in both panels.

For this value of y and 63 efolds of inflation during the slow-roll, fast-roll ends by $\tau = \tau_{trans} = 0.2487963\ldots$. In figures 3, we depict $\log a(\tau)$, $\log h(\tau)$, $\phi(\tau)$, $\log|\dot{\phi}(\tau)|$, $\log[N\ \epsilon_v(\tau)]$ and $p(\tau)/\rho(\tau)$ vs. τ till a short time after the end of inflation. We define the time τ_{end} when inflation ends by the condition $\ddot{a}(\tau_{end}) = 0$ which gives $(\tau_{end} - \tau_*) = 18.2547816\ldots$.

Furthermore, we study in this paper the curvature and tensor fluctuations during the **whole** inflaton evolution in its three succesive regimes: non-inflationary fast-roll, inflationary fast-roll and inflationary slow-roll.

The equation for the scalar curvature fluctuations take in conformal time η and dimensionless variables the form [2]

$$\left[\frac{d^2}{d\eta^2} + k^2 - W_{\mathcal{R}}(\eta)\right] S_{\mathcal{R}}(k;\eta) = 0\,. \tag{2.24}$$

where $d\eta = d\tau/a(\tau)$,

$$W_{\mathcal{R}}(\eta) \equiv \frac{1}{z}\,\frac{d^2 z}{d\eta^2} \quad \text{and} \quad z(\eta) \equiv \frac{a(\eta)}{h(\eta)}\,\frac{d\phi}{d\tau}\,. \tag{2.25}$$

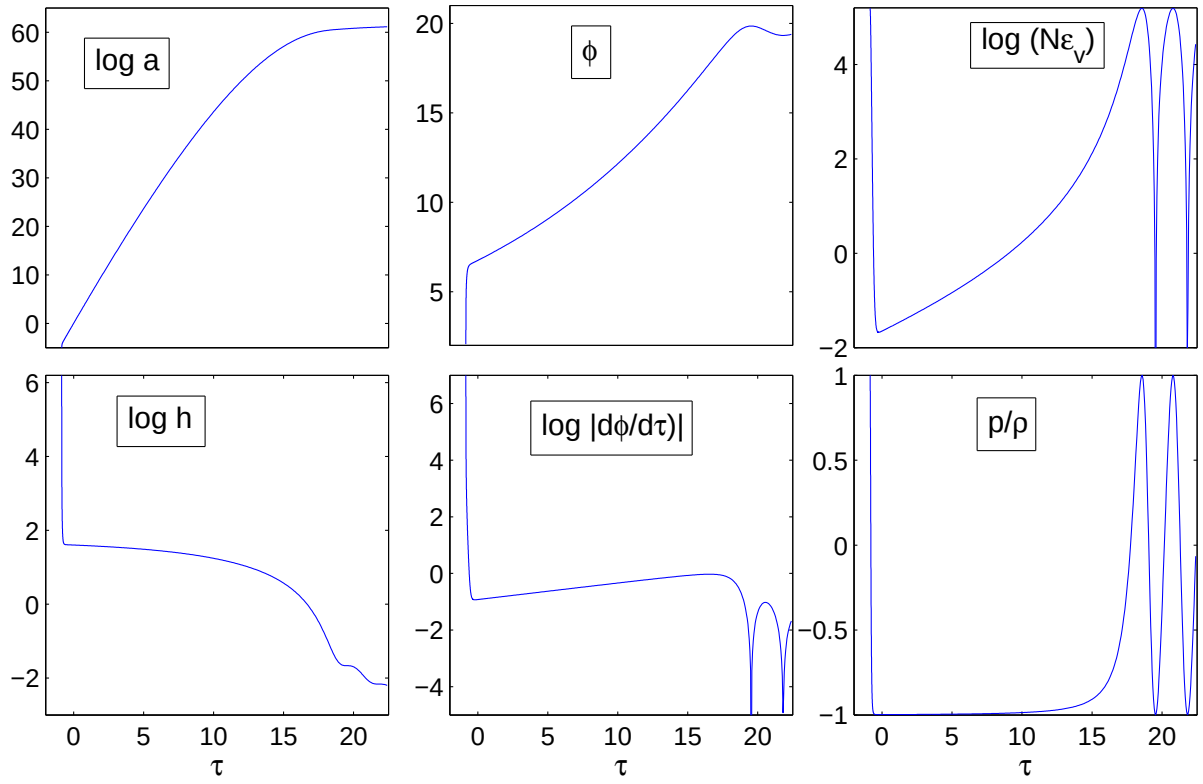

FIG. 3: Time evolution during during the three eras: non-inflationary fast-roll, inflationary fast-roll and slow-roll and beyond the end of inflation (MD era). $\log a(\tau)$, $\log h(\tau)$, $\phi(\tau)$, $\log|\dot{\phi}(\tau)|$, $\log[N\ \epsilon_v(\tau)]$ and $p(\tau)/\rho(\tau)$ vs. τ. $a(\tau)$ grows monotonically reaching 63 efolds by the end of inflation. $h(\tau)$ diverges for $\tau \to \tau_* = -0.8499574\ldots$ according to eq.(2.14) and decreases fast during fast-roll ($\tau \leq \tau_{trans} = 0.2487963\ldots$). Then, $h(\tau)$ decreases slowly during slow-roll as discussed in sec. III B. We depict $h(\tau)$ for short times ($0 < \tau - \tau_* < 0.3$) in fig. 5. $\dot{\phi}(\tau)$ diverges for $\tau \to \tau_*$ according to eq.(2.14) and decreases fast during fast-roll becoming very small during slow-roll. After the fast-roll stage where the inflaton field grows according to eq.(2.14), $\phi(\tau)$ slowly rolls toward its absolute minimum at $\phi_{end} = \sqrt{8\,N/y} = 19.52\ldots$. $\log[N\ \epsilon_v(\tau)]$ vs. $\tau - \tau_*$. We have that $\epsilon_v(\tau_*) = 3$ according to eqs.(2.14) and (2.19). $\epsilon_v(\tau)$ decreases fast during fast-roll becoming of the order $1/N$. We **define** the end of fast-roll (and beginning of slow-roll) by the condition $N\ \epsilon_v(\tau) \equiv 1$ which gives $\tau_{trans} - \tau_* = 0.2487963\ldots$. The equation of state $p(\tau)/\rho(\tau)$ fastly decreases during fast-roll from the value $p/\rho = +1$ for $\tau \to \tau_*$ [see eq.(2.15)] passing through $p/\rho = -1/3$ at the beginning of fast-roll inflation [see eq.(2.12)], $\tau = \tau_s = \tau_* + 0.0573$, and reaching $p/\rho = -1$ by the beginning of slow-roll. p/ρ vanishes again near the end of slow-roll inflation by $\tau_{end} = \tau_* + 18.698\ldots$.

In cosmic time τ, eq.(2.24) takes the form

$$\left[\frac{d^2}{d\tau^2} + h(\tau)\ \frac{d}{d\tau} + \frac{k^2}{a^2(\tau)} - V_{\mathcal{R}}(\tau)\right] S_{\mathcal{R}}(k;\tau) = 0\ . \tag{2.26}$$

where

$$V_{\mathcal{R}}(\tau) \equiv \frac{W_{\mathcal{R}}(\tau)}{a^2(\tau)} = h^2(\tau)\ \left[2 - 7\ \epsilon_v + 2\ \epsilon_v^2 - \sqrt{8\ \epsilon_v}\ \frac{v'(\phi)}{h^2(\tau)} - \eta_v\ (3 - \epsilon_v)\right] =$$
$$= h^2(\tau)\ \left[2 - 7\ \epsilon_v + 2\ \epsilon_v^2\right] - 2\ \frac{d\phi}{d\tau}\ \frac{v'(\phi)}{h(\tau)} - v''(\phi) \quad , \tag{2.27}$$

and ϵ_v and η_v are given by eq.(2.19).

We display $V_{\mathcal{R}}(\tau)$ vs. τ in fig. 4 for the best fit value of the coupling $y = 1.26$ and 63 efolds of slow-roll inflation.

The equation for the tensor fluctuations take in conformal time η and dimensionless variables the form [2]

$$S_T^{''}(k;\eta) + \left[k^2 - \frac{a''(\eta)}{a(\eta)}\right] S_T(k;\eta) = 0\ . \tag{2.28}$$

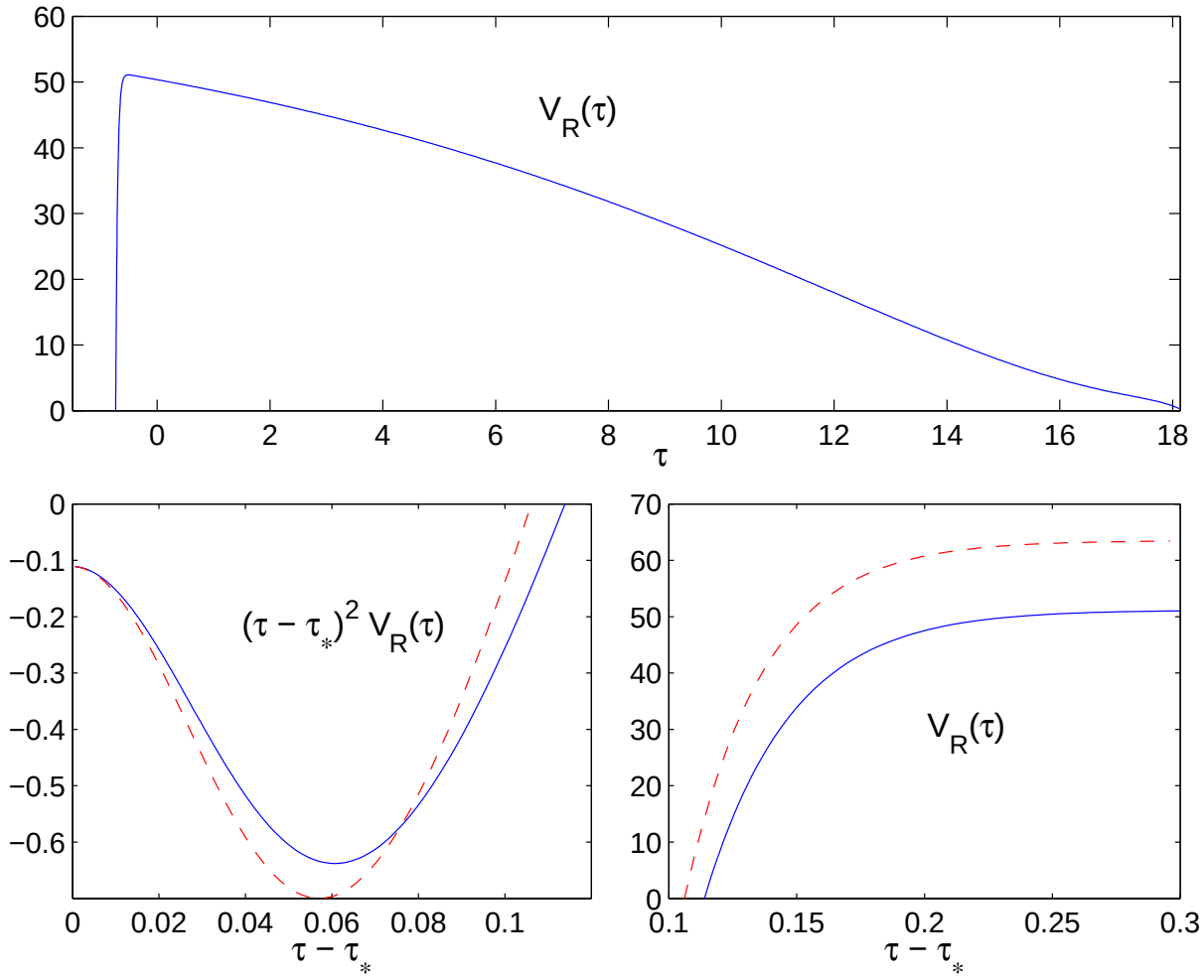

FIG. 4: The potential $V_{\mathcal{R}}(\tau)$ felt by the fluctuations. Upper plot: $V_{\mathcal{R}}(\tau)$ vs. $(\tau - \tau_*)$ in the stage where $V_{\mathcal{R}}(\tau)$ is **repulsive** ($V_{\mathcal{R}}(\tau) > 0$) which happens for $(\tau - \tau_*) > 0.114$. Notice that $V_{\mathcal{R}}(\tau)$ slowly decreases during the slow-roll stage as $V_{\mathcal{R}}(\tau) \simeq 2\ h^2(\tau) + 1 + O(1/N)$ according to eq.(2.27) and fig. 3. Lower plots: Comparison of the exact (numerical) evolution and the analytic approximations eq.(2.43) during fast-roll and slow-roll. Left lower plot: $(\tau - \tau_*)^2\ V_{\mathcal{R}}(\tau)$ vs. $\tau - \tau_*$ in the stage where $V_{\mathcal{R}}(\tau)$ is **atractive** ($V_{\mathcal{R}}(\tau) < 0$) from the exact (numerical) calculation and from the analytic approximation eq.(2.43). This happens for $0 \leq (\tau - \tau_*) < 0.114$. Notice that $\lim_{\tau \to \tau_*} (\tau - \tau_*)^2\ V_{\mathcal{R}}(\tau) = -1/9$ according to eq.(4.1). Lower right plot: $V_{\mathcal{R}}(\tau)$ vs. $\tau - \tau_*$ when $V_{\mathcal{R}}(\tau) > 0$ from the exact (numerical) calculation and from the analytic approximation eq.(2.43).

B. Inflaton and scale factor behaviour near the initial mathematical singularity

In order to find the behaviour of $\phi(\tau)$ and $a(\tau)$ near the initial singularity we write

$$\phi(\tau) = \sqrt{\frac{2}{3}}\ \log\frac{\tau - \tau_*}{b} + \phi_1(\tau) \quad , \quad h(\tau) = \frac{1}{3\ (\tau - \tau_*)} + h_1(\tau)\ . \tag{2.29}$$

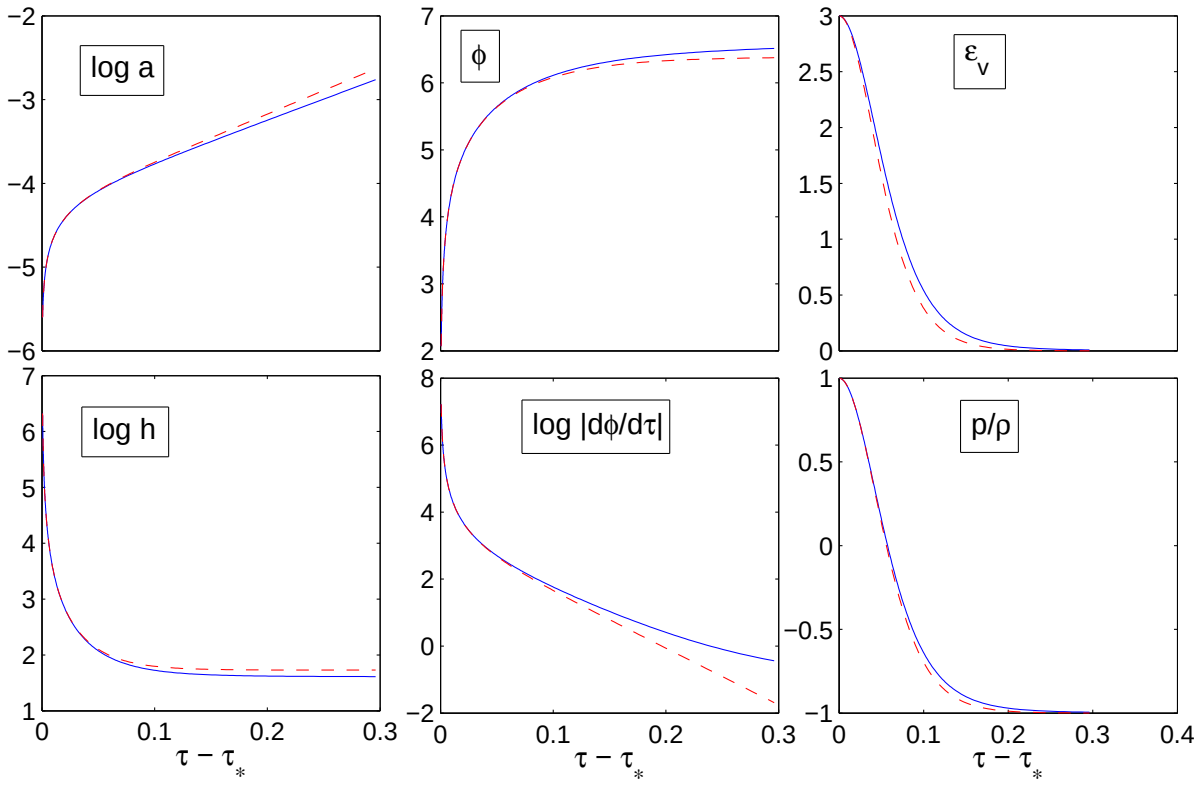

FIG. 5: Comparison of the exact (numerical) evolution (blue continuous line) and the analytic approximations (red dashed line) eq.(2.40) during fast-roll and slow-roll for $\log a(\tau)$, $\log h(\tau)$, $\phi(\tau)$, $\log|\dot\phi(\tau)|$, $\epsilon_v(\tau)$ and $p(\tau)/\rho(\tau)$ vs. $\tau-\tau_*$. The exact $\ln a(\tau)$ and $\ln h(\tau)$ are close to the approximation eq.(2.40). The scale factor is normalized to unit at $\tau=0$, sixty efolds before the end of inflation. The exact (numerical) equation of state $p(\tau)/\rho(\tau)$ is quite close to the analytic approximation eq.(2.42) both during fast-roll and slow-roll. The same happens for the exact (numerical) inflaton field $\phi(\tau)$, $\dot\phi(\tau)$ and the analytic approximation eq.(2.37).

Inserting now eqs.(2.29) into eqs.(2.14) yields for $\phi_1(\tau)$ and $h_1(\tau)$ the non-autonomous differential equations

$$\ddot\phi_1+\left(\frac{1}{\tau-\tau_*}+3\,h_1\right)\dot\phi_1+\frac{\sqrt{6}}{\tau-\tau_*}\,h_1-\phi_1-\sqrt{\frac{2}{3}}\,\log\frac{\tau-\tau_*}{b}+g\left(\sqrt{\frac{2}{3}}\,\log\frac{\tau-\tau_*}{b}+\phi_1\right)^3=0 \tag{2.30}$$

$$h_1^2+\frac{2}{3\,(\tau-\tau_*)}\,h_1-\frac{\dot\phi_1}{6}\left(\sqrt{\frac{2}{3}}\,\frac{2}{\tau-\tau_*}+\dot\phi_1\right)+\frac{1}{6}\left(\sqrt{\frac{2}{3}}\,\log\frac{\tau-\tau_*}{b}+\phi_1\right)^2-\frac{g}{12}\left(\sqrt{\frac{2}{3}}\,\log\frac{\tau-\tau_*}{b}+\phi_1\right)^4-\frac{1}{12\,g}=0\,,$$

where $\dot\phi$ stands for $d\phi/d\tau$.

The asymptotic solution of eqs.(2.30) for $\tau\to\tau_*$ turns to have the dominant form

$$\phi_1(\tau)\stackrel{\tau\to\tau_*}{=}(\tau-\tau_*)^2\,P_4^\phi\left(\log\frac{\tau-\tau_*}{b}\right)\quad,\quad h_1(\tau)\stackrel{\tau\to\tau_*}{=}(\tau-\tau_*)\,P_4^h\left(\log\frac{\tau-\tau_*}{b}\right) \tag{2.31}$$

where $P_4^\phi(z)$ and $P_4^h(z)$ are fourth degree polynomials in their arguments. The polynomials turn to be of fourth degree because the inflaton potential is of fourth degree. Their explicit expressions follow after calculation

$$\phi_1(\tau)\stackrel{\tau\to\tau_*}{=}-\frac{(\tau-\tau_*)^2}{\sqrt{6}}\left[\frac{g}{18}\left(\log^4\frac{\tau-\tau_*}{b}+\frac{2}{3}\,\log^3\frac{\tau-\tau_*}{b}-\frac{11}{3}\,\log^2\frac{\tau-\tau_*}{b}+\frac{49}{9}\,\log\frac{\tau-\tau_*}{b}-\frac{439}{54}\right)\right.$$
$$\left.-\frac{1}{6}\left(\log^2\frac{\tau-\tau_*}{b}+\frac{1}{3}\,\log\frac{\tau-\tau_*}{b}-\frac{7}{8}\right)+\frac{1}{8\,g}\right]\,,$$

$$h_1(\tau) \stackrel{\tau\to\tau_*}{=} \frac{\tau-\tau_*}{9}\left[\frac{g}{18}\left(6\ \log^4\frac{\tau-\tau_*}{b} - 8\ \log^3\frac{\tau-\tau_*}{b} + 8\ \log^2\frac{\tau-\tau_*}{b} - \frac{11}{3}\ \log\frac{\tau-\tau_*}{b} + \frac{146}{9}\right)\right.$$
$$\left. - \log^2\frac{\tau-\tau_*}{b} + \frac{2}{3}\ \log\frac{\tau-\tau_*}{b} - \frac{1}{9} + \frac{3}{4\,g}\right] \tag{2.32}$$

As a consequence, the scale factor near the singularity takes the form

$$a(\tau) \stackrel{\tau\to\tau_*}{=} C\ (\tau-\tau_*)^{\frac{1}{3}}\left[1 + (\tau-\tau_*)^2\ P_4^a\left(\log\frac{\tau-\tau_*}{b}\right)\right]\ . \tag{2.33}$$

where the coefficients of the fourth order polynomial P_4^a can be obtained from eqs.(2.14) and (2.32).

C. Quantum loop effects and the validity of the classical inflaton picture

When $\tau \to \tau_*$ quantum loop corrections are expected to become very large spoiling the classical description. More precisely, quantum loop corrections are of the order $(H/M_{Pl})^2$ [2]. From eqs.(2.7) and (2.14) the quantum loop corrections are of the order

$$\left(\frac{H}{M_{Pl}}\right)^2 \stackrel{(\tau-\tau_*)\ll 1}{=} \left[\frac{m}{3\ (\tau-\tau_*)\ M_{Pl}}\right]^2 = \left(\frac{1.66\ 10^{-6}}{\tau-\tau_*}\right)^2 = \frac{1}{9}\ \left(\frac{\tau_{Planck}}{\tau-\tau_*}\right)^2$$

where we used $m = 1.21\ 10^{13}$ GeV [2].

The characteristic time is here the Planck time

$$\tau_{Planck} = m\ t_{Planck} = \frac{m}{M_{Pl}} = 2.703\ 10^{-43}\ \text{sec} \times m = 4.97\ 10^{-6}\ .$$

Namely, the quantum loop corrections are less than 1% for times

$$(\tau-\tau_*) > \frac{10}{3}\ \tau_{Planck} = 1.66\ 10^{-5}\ . \tag{2.34}$$

Therefore, for times $(\tau-\tau_*) > 10^{-5}$ the classical treatment of the inflaton and the space-time presented in sec. II and II B can be trusted and we see that the classical description has a wide domain of validity.

The use of a classical and homogeneous inflaton field is justified in the out of equilibrium field theory context as the quantum formation of a condensate during inflation. This condensate turns to obey the classical evolution equations of an homogeneous inflaton [11].

We see from eq.(2.14) that the inflaton field becomes negative for $\tau \to \tau_*$. But since a condensate field should be always positive, the classical and homogeneous inflaton picture requires

$$\tau - \tau_* > b$$

For the best fit coupling $y = 1.26$ and 63 efolds of inflation we have $b = 4.745272\ldots\ 10^{-5} = 9.55\ \tau_{Planck}$ which is consistent with eq.(2.34). By comparing this value of b with eq.(2.34) we see that the quantum loop corrections are negligible in the stage where the condensate is already formed.

We can obtain a lower bound on b since b increases with the number of inflation efolds N_{sr} at fixed inflaton potential and since N_{sr} cannot be smaller than the lower bound provided by flatness and entropy [2].

Although all inflationary solutions obtained evolving backwards in time from the slow-roll stage do reach a zero of the scale factor, such mathematical singularity is attained extrapolating the classical treatment where it is **no more valid**. In fact, one never reaches the singularity in the validity region of the classical treatment. In summary, the classical singularity at $\tau = \tau_*$ **is not a real physical phenomenon** here.

The classical description with the homogeneous inflaton is very good for $\tau - \tau_* > 10\ \tau_{Planck}$ well before the beginning of inflation.

D. The fast-roll regime: analytic approach

As we see from fig. 3 the inflaton field $\phi(\tau)$ is much smaller than $d\phi/d\tau$ during fast-roll. We can therefore approximate the coupled inflaton evolution equation and Friedmann equation eqs.(2.11) as

$$\frac{d^2\phi}{d\tau^2} + 3\,h\,\frac{d\phi}{d\tau} = 0 \quad ,$$
$$h^2(\tau) = \frac{1}{3}\left[\frac{1}{2}\left(\frac{d\phi}{d\tau}\right)^2 + \frac{1}{4\,g}\right] \quad . \tag{2.35}$$

Or, in a compact form,

$$\frac{d^2\phi}{d\tau^2} + \sqrt{\frac{3}{2}}\,\frac{d\phi}{d\tau}\,\sqrt{\left(\frac{d\phi}{d\tau}\right)^2 + \frac{1}{2\,g}} = 0\,, \tag{2.36}$$

which has the exact solution

$$\frac{d\phi}{d\tau} = \sqrt{\frac{2}{3}}\,\frac{1}{\tau_1\,\sinh\left(\frac{\tau-\tau_*}{\tau_1}\right)} \quad , \quad \phi(\tau) = \sqrt{\frac{2}{3}}\,\log\left[\frac{2\,\tau_1}{b}\,\tanh\left(\frac{\tau-\tau_*}{2\,\tau_1}\right)\right] \quad , \tag{2.37}$$

where τ_1 turns out to be the characteristic time scale

$$\tau_1 = 2\,\sqrt{\frac{g}{3}} = \sqrt{\frac{y}{6\,N}}\,. \tag{2.38}$$

We find for the best fit to CMB and LSS data, $y = 1.26$ and $N = 60$,

$$\tau_1 = 0.0592 = 11910\,\tau_{Planck}\,, \tag{2.39}$$

well after the Planck scale $\tau_{Planck} = 4.97\,10^{-6}$.

The integration constant in eq.(2.37) matches with the small $\tau - \tau_*$ behaviour eq.(2.14). The Hubble parameter and the scale factor are here

$$h(\tau) = \frac{1}{3\,\tau_1}\,\coth u \quad , \quad a(\tau) = C\,\left[\tau_1\,\sinh u\right]^{\frac{1}{3}} \quad , \quad u \equiv \frac{\tau-\tau_*}{\tau_1} \quad , \tag{2.40}$$

where the integration constant was chosen to fulfil eq.(2.16). The scale factor eq.(2.40) interpolates between the non-inflationary power law behaviour eq.(2.16) for $\tau - \tau_* \to 0$ and the eternal inflationary de Sitter behaviour for $\tau - \tau_* \gg \tau_1$. Since we have set $v(\phi)$ equal to constant, slow-roll De Sitter inflation **never stops** in this approximation. Namely, neither matter-dominated nor radiation-dominated eras are reached in this approximation.

We can eliminate the variable u between ϕ and $d\phi/d\tau$ in eq.(2.37) with the result

$$\frac{d\phi}{d\tau} = \sqrt{\frac{2}{3}}\,\left[\frac{e^{-\sqrt{\frac{3}{2}}\,\phi(\tau)}}{b} - \frac{b}{4\,\tau_1^2}\,e^{\sqrt{\frac{3}{2}}\,\phi(\tau)}\right]\,. \tag{2.41}$$

This equation generalizes eq.(2.18) which corresponds to the first term here and describes the behaviour for $\tau - \tau_*$. Notice that

$$-\infty < \phi(\tau) < \sqrt{\frac{2}{3}}\,\log\left[\frac{2\,\tau_1}{b}\right] \quad , \quad 0 < \frac{d\phi}{d\tau} < +\infty$$

and that $b/[2\,\tau_1] = 4.0105\,10^{-4}$.

The evolution described by eqs.(2.37)-(2.40) starts from the mathematical singularity at $\tau = \tau_*$ with monotonically decreasing $d\phi/d\tau$ and $h(\tau)$ and a monotonically increasing $\phi(\tau)$ from its initial value $\phi(\tau_*) = -\infty$.

Slow-roll is reached asymptotically for large τ since $d\phi/d\tau$ vanishes for $\tau - \tau_* \to \infty$.

We find for the parameter ϵ_v [eq. (2.19)] and for the equation of state,

$$\epsilon_v(\tau) = \frac{3}{1+\sinh^2 u} \quad , \quad \frac{p(\tau)}{\rho(\tau)} = \frac{2}{\cosh^2 u} - 1 \quad . \tag{2.42}$$

We see that $\epsilon_v(\tau)$ monotonically decreases with τ and vanishes for $\tau - \tau_* \to \infty$. The equation of state p/ρ smoothly interpolates between $+1$ at $\tau = \tau_*$ (extreme non-inflationary fast-roll) and -1 (slow-roll inflation) for $\tau - \tau_* \to \infty$, passing by $p/\rho = -1/3$ (the beginning of fast-roll inflation) at $\tau - \tau_* = 0.0573$.

The potential $V_{\mathcal{R}}(\tau)$ eq.(2.24) felt by the fluctuations takes here the form

$$V_{\mathcal{R}}(\tau) = \frac{1}{6\,g}\left[1 - \frac{1}{2\,\sinh^2 u} - \frac{9}{\cosh^2 u}\right] \quad , \quad u = \frac{\tau - \tau_*}{\tau_1} \, . \tag{2.43}$$

The limiting values of $h(\tau)$, $\phi(\tau)$ and $V_{\mathcal{R}}(\tau)$ for $\tau \to \infty$ give a reasonable approximation to the numerical results. We have

$$h(\infty) = \frac{1}{3\,\tau_1} = \sqrt{\frac{2\,N}{3\,y}} \quad , \quad \phi(\infty) = \sqrt{\frac{2}{3}}\,\log\left[\frac{2\,\tau_1}{b}\right] \quad , \quad \frac{d\phi}{d\tau}(\infty) = 0 \quad , \quad V_{\mathcal{R}}(\infty) = \frac{4\,N}{3\,y} \, . \tag{2.44}$$

The characteristic time scale τ_1 is generically a small number since according to eq.(2.38) $\tau_1 \sim 1/\sqrt{N}$. The value of τ_1 for the best fit value for y is given in eq.(2.39).

The end of fast-roll τ_{trans} can be estimated in this approximation by using eq.(2.42) for $\epsilon_v(\tau)$ setting $\epsilon_v(\tau_{trans}) = 1/N$. This gives,

$$\epsilon_v(\tau) \simeq 12\,e^{-\frac{2\,\tau_{trans}}{\tau_1}} = \frac{1}{N} \quad , \quad \tau_{trans} \simeq \frac{1}{2}\,\tau_1\,\ln(12\,N) = 0.195 \, .$$

This approximated value for τ_{trans} should be compared with the exact numerical result $\tau_{trans} = 0.2487963\ldots$. $h(\tau_{trans})$ and $V_{\mathcal{R}}(\tau_{trans})$ differ in less than 1% from their values at $\tau = \infty$ given by eq.(2.44).

In figs. 5 we plot $\ln a(\tau)$, $\ln h(\tau)$, $\phi(\tau)$, $\ln|\dot{\phi}(\tau)|, \epsilon_v(\tau)$ and $p(\tau)/\rho(\tau)$ computed **numerically** and computed using the analytic expressions eqs.(2.37)-(2.42). We compare in figs. 4 the exact potential $V_{\mathcal{R}}(\tau)$ with the analytic approximation eq.(2.43).

We see that the simple analytic formulas eqs.(2.37)-(2.43) provide a very good approximation during the fast-roll regime $\tau \leq t_{trans} = 0.2487963\ldots$. In particular, eq.(2.37) provides an excellent approximation to $\phi(\tau)$ as shown in fig. 5. In particular, the analytic formulas eqs.(2.37)-(2.43) become **exact** near the singularity at $\tau = \tau_*$.

E. The fast-roll regime: numerical solution

To construct a singular solution we can integrate eqs. (2.11) backwards in time starting from initial conditions of strong non-inflationary fast–roll type, namely

$$K \equiv \frac{\dot{\phi}^2}{2\,v(\phi)} \gg 1 \, ,$$

producing a given total number N_{sr} of slow–roll inflationary efolds. For instance, we start from some ϕ and $\dot{\phi}$ such that $K = 10^4$. The time extent backwards from this moment has to be limited so that, integrating back and forth, the required relative accuracy of 10^{-12} is preserved. We furthermore impose that $N_{sr} = 63$.

We adopt the convention that conformal time η vanishes from below when inflation ends and that $a(\tau = 0) = 1$ when there are still $N = 60$ efolds till the end of inflation. This choice of the scale factor normalization seems the most natural. Then, η has a finite non-zero limit η_* as τ approaches the time τ_* of the singularity, since $a(\tau) \simeq C\,(\tau - \tau_*)^{1/3}$ as $\tau \to \tau_*$ according to eq.(2.16). That is,

$$\eta = \int_{\tau_{end}}^{\tau} \frac{d\tau'}{a(\tau')} = \eta_* + \int_{\tau_*}^{\tau} \frac{d\tau'}{a(\tau')} \, .$$

The numerics of a fast–roll solution of this type are in Table I where a relative accuracy of 10^{-12} is preserved.

Using the asymptotic behaviour eq.(2.14) as $\tau \to \tau_*^+$ we obtain from Table I:

$$\tau_* = -0.8499574\ldots \quad , \quad b = 4.745272\ldots 10^{-5} \quad \text{and} \quad \eta_* = -15.605614\ldots \ .$$

Slow–roll begins at $\tau_{trans} = \tau_* + 0.2487963\ldots = -0.6011611\ldots$.

The initial value of the ratio

$$\frac{d\varphi/dt}{\varphi} = m\,\frac{\dot\phi}{\phi}$$

has the dimension of mass. The natural mass scale in the problem is here the energy scale of inflation M. Therefore, assuming this ratio of the order M yields

$$\frac{\dot\phi}{\phi} < \frac{M}{m} \sim 10^3 \ .$$

Hence, it s natural to start the fast–roll evolution with $\dot\phi/\phi < 10^3$.

	$K = 5.3458\ldots\ 10^7$	$K = 10^4$	inflation start: $\ddot a = 0^-$	fast-roll $\to$ slow-roll	$a = 1$	inflation end: $\ddot a = 0^+$
τ	$-0.8499493\ldots$	$-0.8493593\ldots$	$-0.7746494\ldots$	$-0.6011611\ldots$	0	$17.4048242\ldots$
ϕ	$-1.4401237\ldots$	$2.0690604\ldots$	$5.9342489\ldots$	$6.4783577\ldots$	$6.7484076\ldots$	$18.5586530\ldots$
$\dot\phi$	$100391.035\ldots$	$1365.05241\ldots$	$8.8601670\ldots$	$0.9182661\ldots$	$0.3974015\ldots$	$0.94150557\ldots$
$\log a$	$-7.0325621\ldots$	$-5.5999353\ldots$	$-3.9142151\ldots$	$-2.9999999\ldots$	0	60
h	$40984.4689\ldots$	$557.30817\ldots$	$6.2650841\ldots$	$5.0295509\ldots$	$4.9653990\ldots$	$0.6657449\ldots$
η	$-15.6050091\ldots$	$-15.376218\ldots$	$-15.3549996\ldots$	$-4.0169827\ldots$	$-0.2020609\ldots$	0

TABLE I: Fast-roll solution with $N_{sr} = 63$ efolds of slow-roll inflation. Recall that $\tau = 4.97\ 10^{-6}\ (t/t_{Planck})$.

III. THE SLOW-ROLL INFLATIONARY ERA

A. The extreme slow-roll solution

There always exist a special solution of eqs.(2.11) that starts at $\tau = -\infty$ with vanishing inflaton, vanishing scale factor but nonzero Hubble parameter. More precisely, eqs.(2.11) can be approximated for small ϕ and $\dot\phi$ as

$$\begin{aligned} &\frac{d^2\phi}{d\tau^2} + 3\,h\,\frac{d\phi}{d\tau} - \phi = 0 \quad , \\ &h^2(\tau) = \frac{1}{3}\,v(0) \quad . \end{aligned} \tag{3.1}$$

where we used eqs.(2.9) and (2.11).

Eqs.(3.1) admit the asymptotic solution for $\tau \to -\infty$

$$\phi(\tau) \stackrel{\tau\to-\infty}{=} C_0\,e^{\alpha\,\tau} \to 0 \quad , \quad h(\tau) \stackrel{\tau\to-\infty}{=} \sqrt{\frac{v(0)}{3}} \quad , \quad a(\tau) \stackrel{\tau\to-\infty}{=} e^{\sqrt{\frac{v(0)}{3}}\,\tau} \to 0 \ , \tag{3.2}$$

where C_0 is an integration constant, $v(0) = 2\,N/y$ for the double-well potential eq.(2.23) and

$$\alpha \equiv \frac{1}{2}\left[\sqrt{3\,v(0)+4} - \sqrt{3\,v(0)}\right] > 0 \ .$$

Notice that α can be expressed in terms of the fast-roll characteristic time-scale τ_1 [eq.(2.38)],

$$\alpha = \frac{1}{2\,\tau_1}\left[\sqrt{1+4\,\tau_1^2} - 1\right] \simeq \tau_1$$

since $\tau_1 \simeq 0.0592 \ll 1$ [see eq.(2.39)].

It must be noticed that the characteristic time scale of the inflaton evolution in the extreme slow-roll solution for early times [see eq.(3.2)]

$$\frac{1}{\alpha} \simeq \frac{1}{\tau_1} \gg 1 \; ,$$

turns to be the **inverse** of the characteristic time scale τ_1 of the fast-roll solution and to be very large.

On the contrary, the characteristic time scale of the scale factor evolution in the same regime is very short

$$\sqrt{\frac{3}{v(0)}} = 3\,\tau_1 \ll 1 \; .$$

The fast-roll stages both non-inflationary and inflationary are absent in this solution. The extreme slow-roll solution only possesses the slow-roll inflationary stage followed by the matter dominated era.

	inflation start	$a = 1$	inflation end: $\ddot{a} = 0^+$
τ	$-344.9514017\ldots$	0	$17.40482446\ldots$
ϕ	10^{-8}	$6.7484118\ldots$	$18.5586530\ldots$
$\dot{\phi}$	$\alpha\, 10^{-8} = 5.8937108453...10^{-10}$	$0.3973384\ldots$	$0.94150557\ldots$
$\log a$	$-1938.4867948\ldots$	0	60
h	$\sqrt{2\,N/(3\,y)} = 5.6361006\ldots$	$4.9653973\ldots$	$0.6657449\ldots$
η	$-\infty$ (f.a.p.p)	$-0.2020610\ldots$	0

TABLE II: Relevant quantities of the extreme slow-roll inflaton solution for the coupling $y = 1.2592226\ldots$. We adopt the convention that $a(\tau = 0) = 1$ when there are still $N = 60$ efolds till the end of inflation. Recall that $\tau = 4.97\ 10^{-6}\ (t/t_{Planck})$.

For the value of the coupling $y = 1.2592226\ldots$, we get for the extreme slow–roll solution

$$\alpha = 0.058937108\ldots \; , \quad \phi_{\rm end} = 18.5586530\ldots \; , \quad \dot{\phi}_{\rm end} = 0.9415055\ldots \tag{3.3}$$

In table II we display the values of the relevant magnitudes for this extreme slow-roll solution.

Except for the extreme slow–roll solution, all solutions are of fast-roll type and come from singular values of ϕ and h according to eq.(2.14) as $\tau \to \tau_*^+$ for some finite τ_* characteristic of each particular solution. The slow-roll stage (which starts when $\epsilon_v = 1/N$ from above, and ends when again $\epsilon_v = 1/N$ from below) of all distinct solutions turns to be almost identical to that of the extreme slow–roll case as one could expect for an attractor.

B. The inflaton during slow-roll inflation: analytical solution

In the slow-roll regime higher time derivatives can be neglected in the evolution eqs.(2.11) with the result

$$3\,h(\tau)\,\dot{\phi} + v'(\phi) = 0 \quad , \quad h^2(\tau) = \frac{v(\phi)}{3} \; . \tag{3.4}$$

These first order equations can be solved in closed form as

$$N[\phi] = -\int_{\phi}^{\phi_{end}} v(\phi')\,\frac{d\phi'}{dv}\,d\phi' \; . \tag{3.5}$$

where $N[\phi]$ is the number of e-folds since the field ϕ exits the horizon till the end of inflation (where it takes the value ϕ_{end}).

Eq.(3.5) indicates that $N[\phi]$ scales as ϕ^2 and hence the field ϕ is of the order $\sqrt{N} \sim \sqrt{60}$. Therefore, we proposed as universal form for the inflaton potential [2, 10]

$$v(\varphi) = N\,M^4\,w(\chi) \; , \tag{3.6}$$

where χ is the dimensionless, slowly varying field

$$\chi = \frac{\varphi}{\sqrt{N}\, M_{Pl}} = \frac{\phi}{\sqrt{N}} \, . \tag{3.7}$$

The equations of motion (2.11) in the field χ become

$$\begin{aligned} &\mathcal{H}^2(\hat{\tau}) = \frac{1}{3}\left[\frac{1}{2\,N}\left(\frac{d\chi}{d\hat{\tau}}\right)^2 + w(\chi)\right] \quad \text{with} \quad \mathcal{H} = \frac{h}{\sqrt{N}} \, , \\ &\frac{1}{N}\,\frac{d^2\chi}{d\hat{\tau}^2} + 3\,\mathcal{H}\,\frac{d\chi}{d\hat{\tau}} + w'(\chi) = 0 \quad . \end{aligned} \tag{3.8}$$

and $\hat{\tau}$ stands for the rescaled dimensionless time

$$\hat{\tau} \equiv \frac{\tau}{\sqrt{N}} = \frac{m\,t}{\sqrt{N}} \, .$$

To leading order in the slow-roll approximation (neglecting $1/N$ corrections), eqs.(3.8) are solvable in terms of quadratures

$$\hat{\tau} - \hat{\tau}_{trans} = -\int_{\chi(\hat{\tau}_{trans})}^{\chi} d\chi' \, \frac{\sqrt{3\,w(\chi')}}{w'(\chi')} \, , \tag{3.9}$$

where $\hat{\tau}_{trans}$ stands for the beginning of slow-roll inflation and we used that

$$\mathcal{H}(\hat{\tau}) = \sqrt{\frac{w(\chi)}{3}} + \mathcal{O}\left(\frac{1}{N}\right) \, , \tag{3.10}$$

For the broken symmetric potential eq.(2.20), from eqs.(2.10), (3.9) and (3.10), we find

$$\chi(\hat{\tau}) = \chi(\hat{\tau}_{trans})\, e^{\sqrt{\frac{y}{6}}\,(\hat{\tau}-\hat{\tau}_{trans})} + \mathcal{O}\left(\frac{1}{N}\right) = \sqrt{\frac{8}{y}}\, e^{-\sqrt{\frac{y}{6}}\,(\hat{\tau}_{end}-\hat{\tau})} + \mathcal{O}\left(\frac{1}{N}\right) \, , \tag{3.11}$$

$$\begin{aligned} &\mathcal{H}(\hat{\tau}) = \sqrt{\frac{2}{3\,y}}\left[1 - e^{-\sqrt{\frac{2\,y}{3}}\,(\hat{\tau}_{end}-\hat{\tau})}\right] + \mathcal{O}\left(\frac{1}{N}\right) \, , \\ &\frac{p}{\rho}(\hat{\tau}) = -1 + \frac{y}{6\,N}\,\frac{1}{\sinh^2\left[\sqrt{\frac{y}{6}}(\hat{\tau}_{end}-\hat{\tau})\right]} + \mathcal{O}\left(\frac{1}{N^2}\right) \, , \end{aligned} \tag{3.12}$$

$$\text{for} \quad \hat{\tau}_{trans} \leq \hat{\tau} \leq \hat{\tau}_{end} = \sqrt{\frac{3}{2\,y}}\,\ln\left[\frac{8}{\chi^2(\hat{\tau}_{trans})\,y}\right] + \mathcal{O}\left(\frac{1}{\sqrt{N}}\right) \, . \tag{3.13}$$

Inflation ends when the equation of state becomes $p/\rho = -1/3$ [see eq.(2.12)]. According to eq.(3.12), this happens when $\hat{\tau}_{end} - \hat{\tau} \sim \mathcal{O}\left(1/\sqrt{N}\right)$. Therefore, expressions eqs.(3.11)-(3.12) are valid as long as

$$\hat{\tau}_{trans} \leq \hat{\tau} \leq \hat{\tau}_{end} - \mathcal{O}\left(\frac{1}{\sqrt{N}}\right) \quad \text{where} \quad \mathcal{O}\left(\frac{1}{\sqrt{N}}\right) > 0 \, .$$

That is, eqs.(3.11) hold while the inflaton is not very near the minimum of the potential $\chi_{end} = \sqrt{8/y}$.

By integrating the Hubble parameter $\mathcal{H}(\hat{\tau})$ we obtain for the scale factor $a(\hat{\tau})$

$$\begin{aligned} \log\frac{a(\hat{\tau})}{a(\hat{\tau}_{trans})} &= \sqrt{\frac{2}{3\,y}}\,N\,(\hat{\tau}-\hat{\tau}_{trans}) - \frac{N}{8}\,\chi^2(\hat{\tau}_{trans})\left[e^{\sqrt{\frac{2\,y}{3}}\,(\hat{\tau}-\hat{\tau}_{trans})} - 1\right] = \\ &= \sqrt{\frac{2\,N}{3\,y}}\,m\,(t-t_{trans}) - \frac{1}{8}\left[\frac{\varphi(t_{trans})}{M_{Pl}}\right]^2\left[e^{\sqrt{\frac{2\,y}{3\,N}}\,m\,(t-t_{trans})} - 1\right] \, , \end{aligned} \tag{3.14}$$

where we used eqs.(2.7) and (3.11). It must be noticed that $a(\hat{\tau})$ is not exactly a de Sitter scale factor, even in the large N limit at fixed $\hat{\tau}$.

At the end of inflation the number of efolds is $\ln a \simeq 64$, the inflaton is near its minimum

$$\chi = \sqrt{\frac{8}{y}} \simeq 2.52 \quad ,$$

$\dot{\chi}$ starts to oscillate around zero and $\mathcal{H}(\hat{\tau})$ begins a rapid decrease (see figs. 3). At this time the inflaton field is no longer slowly coasting in the $w''(\chi) < 0$ region but rapidly approaching its equilibrium minimum. When inflation ends, the inflaton is at its minimum value up to corrections of order $1/\sqrt{N}$. Therefore, we see from the Friedmann eq.(3.8) and eqs.(3.11) that

$$\frac{1}{N}\left(\frac{d\chi}{d\hat{\tau}}\right)^2(\hat{\tau}_{end}) = \mathcal{O}\left(\frac{1}{N}\right) \quad , \quad w(\chi(\hat{\tau}_{end})) = \mathcal{O}\left(\frac{1}{N}\right) \quad \text{and therefore,} \quad \mathcal{H}(\hat{\tau}_{end}) = \mathcal{O}\left(\frac{1}{\sqrt{N}}\right) , \tag{3.15}$$

while $\mathcal{H}(\hat{\tau}_{trans}) = \mathcal{O}(1)$. Namely, the Hubble parameter decreases by a factor of the order $\sqrt{N} \sim 8$ during slow-roll inflation. We see in fig. 3 that the exact $\mathcal{H}(\hat{\tau})$ decreases by a factor six during slow-roll inflation, confirming the slow-roll analytic estimate.

We can compute the total number of inflation efolds N_{tot} to leading order in slow-roll inserting the analytic formula for $\hat{\tau}_{end}$ eq.(3.13) in eq.(3.14) with the result,

$$N_{tot} = \frac{N}{y}\left\{\ln\left[\frac{8}{\chi^2(\hat{\tau}_{trans})\, y}\right] - 1 + \frac{1}{8}\, y\, \chi^2(\hat{\tau}_{trans})\right\} + \mathcal{O}\left(\frac{1}{\sqrt{N}}\right) . \tag{3.16}$$

We have verified the slow-roll analytical results eqs.(3.11)-(3.16) comparing them with the numerical solution of eqs.(2.11). Both results are concordant up to the error estimation in each case: $\mathcal{O}(1/N)$ or $\mathcal{O}\left(1/\sqrt{N}\right)$.

The field ϕ as a function of the dimensionless time τ eq.(3.11) takes the form

$$\phi(\tau) = \phi(\tau_{trans})\, e^{\sqrt{\frac{y}{6\,N}}\,(\tau - \tau_{trans})}$$

and then

$$\dot{\phi}(\tau) = \sqrt{\frac{y}{6\,N}}\,\phi(\tau) .$$

For $y \simeq 1.26$ and $N = 60$ we get $\sqrt{y/[6\,N]} = 0.0577$ in agreement with the slope of the red quasi-horizontal slow-roll line in the phase space flow fig. 1.

IV. COMPLETE FLUCTUATIONS EVOLUTION AND FAST-ROLL EFFECTS ON THE POWER SPECTRUM.

A. Scalar and tensor fluctuations near the initial singularity.

In order to study the curvature and tensor fluctuations in this regime, it is important to evaluate the parameter ϵ_v and the potential felt by the fluctuations $V_{\mathcal{R}}$.

Inserting eqs.(2.29) and (2.31) into eqs.(2.19) and (2.27) yields near the initial singularity

$$V_{\mathcal{R}}(\tau) \stackrel{\tau\to\tau_*}{=} -\frac{1}{9\,(\tau-\tau_*)^2}\left[1 + (\tau-\tau_*)^2\, P_4^V\left(\log\frac{\tau-\tau_*}{b}\right)\right] \quad , \quad \epsilon_v \stackrel{\tau\to\tau_*}{=} 3\left[1 + (\tau-\tau_*)^2\, P_4^\epsilon\left(\log\frac{\tau-\tau_*}{b}\right)\right] \tag{4.1}$$

$$W_{\mathcal{R}}(\eta) \stackrel{\eta\to 0}{=} -\frac{1}{4\,\eta^2}\left[1 + \eta^3\, P_4^W(\log\eta)\right] . \tag{4.2}$$

where

$$\eta \stackrel{\tau\to\tau_*}{=} \frac{3}{2}\,(\tau-\tau_*)^{\frac{2}{3}}$$

is the conformal time for $\tau \to \tau_*$ and $P_4^V(x)$, $P_4^\epsilon(x)$ and $P_4^W(x)$ are polynomials of degree four in x .

We see that the fluctuations feel a **singular attractive** potential near the $\eta = 0$ singularity. Actually, the behaviour of $W_{\mathcal{R}}(\eta)$ for $\eta \to 0$ is **exactly** the **critical** strength $(-1/4)$ for which the fall to the centre becomes possible in a central and attractive singular potential [3].

We find from eqs.(2.26) and (4.1) for the fluctuations near the singularity

$$S_{\mathcal{R}}(k;\eta) \stackrel{\eta,\eta_0\to 0}{=} \sqrt{\frac{\eta}{\eta_0}} \left[\mathcal{A}_{\mathcal{R}}(k) + \mathcal{B}_{\mathcal{R}}(k)\ \log\frac{\eta}{\eta_0}\right] , \tag{4.3}$$

where η_0 is the time when the initial conditions will be imposed, $\mathcal{A}_{\mathcal{R}}$ and $\mathcal{B}_{\mathcal{R}}$ are complex constants constrained by the Wronskian condition (that ensures the canonical commutation relations) [2]

$$W[S_{\mathcal{R}}, S^*_{\mathcal{R}}] = S_{\mathcal{R}}\ \frac{dS^*_{\mathcal{R}}}{d\eta} - \frac{dS_{\mathcal{R}}}{d\eta}\ S^*_{\mathcal{R}} = i\ . \tag{4.4}$$

Namely,

$$2\ \mathrm{Im}[\mathcal{A}_{\mathcal{R}}\ \mathcal{B}^*_{\mathcal{R}}] = \eta_0\ . \tag{4.5}$$

Precisely, the logarithmic behaviour for $\eta \to 0$ of the wave function eq.(4.3) describes the fall to $\tau - \tau_* = 0$ for the critical strength of the potential $W_{\mathcal{R}}(\eta)$. For larger attractive strengths the wave function eq.(4.3) shows up an oscillatory behaviour [3]. Notice, however the physical nature of the process: here we have a time evolution near a classical singularity at a given time while in the potential case one has particles falling (or emerging) from a point in space where the potential is singular.

In general, the mode functions for large k must behave as free modes (plane waves) since the potential $W_{\mathcal{R}}(\eta)$ in eq.(2.24) becomes negligible in this limit except at the singularity $\tau = \tau_*$. One can then impose Bunch-Davies conditions for large k which corresponds to assume an initial quantum vacuum Fock state, empty of curvature excitations [2]

$$S_{\mathcal{R}}(k;\tau) \stackrel{k\to\infty}{=} \frac{e^{-i\ k\ \eta}}{\sqrt{2\ k}} \tag{4.6}$$

and therefore

$$\frac{dS_{\mathcal{R}}}{d\eta}(k;\eta_0) \stackrel{k\to\infty}{=} -i\ k\ S_{\mathcal{R}}(k;\eta_0)\ .$$

Eq.(4.6) fulfils the Wronskian normalization eq.(4.4).

In asymptotically flat (or conformally flat) regions of the space-time the potential felt by the fluctuations vanish and the fluctuations exhibit a plane wave behaviour for **all** k (not necesarily large). This is not the case near strong gravity fields or curvature singularities as in the present cosmological space-time where $W_{\mathcal{R}}(\eta)$ can never be neglected at fixed k. However, we can choose Bunch-Davies initial conditions (BDic) at $\eta = \eta_0$ by imposing

$$\frac{dS_{\mathcal{R}}}{d\eta}(k;\eta_0) = -i\ k\ S_{\mathcal{R}}(k;\eta_0) \quad \text{for all } k\ . \tag{4.7}$$

That is, we consider the initial value problem for the mode functions giving the values of $S_{\mathcal{R}}(k;\eta)$ and $dS_{\mathcal{R}}/d\eta$ at $\eta = \eta_0$.

Notice that eq.(4.7) combined with the Wronskian condition eq.(4.4) implies that

$$|S_{\mathcal{R}}(k;\eta_0)| = \frac{1}{\sqrt{2\ k}} \quad , \quad \left|\frac{dS_{\mathcal{R}}}{d\eta}(k;\eta_0)\right| = \sqrt{\frac{k}{2}}\ .$$

which is equivalent to eq.(4.6) for large k.

Since the mode functions $S_{\mathcal{R}}(k;\eta)$ are defined up to an arbitrary constant phase we can write eq.(4.3) valid near the metric singularity as

$$S_{\mathcal{R}}(k;\eta) \stackrel{\eta,\eta_0\to 0}{=} \sqrt{\frac{\eta}{2\ k\ \eta_0}} \left[1 - \left(\frac{1}{2} + i\ k\ \eta_0\right)\ \log\frac{\eta}{\eta_0}\right] . \tag{4.8}$$

Inflation (fast-roll) starts	$\ddot{a}(\tau_s) = 0$	$\tau_s = \tau_* + 0.0753090$
$V_{\mathcal{R}}(\tau)$ becomes positive	$V_{\mathcal{R}}(\tau_+) = 0$	$\tau_+ = \tau_* + 0.114$
End of fast-roll	$N\ \epsilon_v(\tau_{trans}) = 1$	$\tau_{trans} = \tau_* + 0.2487963\ldots$
Maximum of $V_{\mathcal{R}}(\tau)$	$V'_{\mathcal{R}}(\tau_M) = 0$	$\tau_M = \tau_* + 0.3503\ ,\ V_{\mathcal{R}}(\tau_M) = 51.196$
End of Inflation	$p(\tau_{end}) = 0$	$\tau_{end} = \tau_* + 18.2547816$

TABLE III: Selected time values for $y = 1.26$ and $N_{sr} = 63$ efolds of slow-roll inflation. Notice that slow-roll starts exactly when fast-roll ends. Recall that $\tau = 4.97\ 10^{-6}\ (t/t_{Planck})$.

In eq.(4.3) this corresponds to the coefficients,

$$\mathcal{A}_{\mathcal{R}} = \frac{1}{\sqrt{2\,k}} \quad , \quad \mathcal{B}_{\mathcal{R}} = \frac{1}{\sqrt{2\,k}} \left(\frac{1}{2} + i\ k\ \eta_0 \right) \quad .$$

We have in cosmic time,

$$S_{\mathcal{R}}(k;\tau) \stackrel{\tau,\tau_0 \to \tau_*}{=} \frac{1}{\sqrt{2\,k}} \left(\frac{\tau - \tau_*}{\tau_0} \right)^{\frac{1}{3}} \left[1 - \left(\frac{1}{3} + i\ k\ \tau_0^{\frac{2}{3}} \right) \log \frac{\tau - \tau_*}{\tau_0} \right] , \tag{4.9}$$

where $\tau_0 - \tau_* = (2\ \eta_0/3)^{\frac{3}{2}}$ for $\tau \to \tau_*$.

Namely, imposing the BD initial condition (BDic) eq.(4.7) at small η_0 where the small η behavior eq.(4.3) applies, yields specific values for the coefficients of the linearly independent solutions $\sqrt{\eta}$ and $\sqrt{\eta}\,\log\eta$ that we can read from eqs.(4.8)-(4.9).

For general τ_0 (i. e., τ_0 not near τ_*), the mode functions for $\tau \to \tau_*$ take the form

$$S_{\mathcal{R}}(k;\tau) \stackrel{\tau \to \tau_*}{=} \frac{1}{\sqrt{2\,k}} \left(\frac{\tau - \tau_*}{\tau_0} \right)^{\frac{1}{3}} \left[X(k,\tau_0) - \left(Y(k,\tau_0) + \frac{i\ k\ \tau_0^{\frac{2}{3}}}{X(k,\tau_0)} \right) \log \frac{\tau - \tau_*}{\tau_0} \right] , \tag{4.10}$$

where we imposed eq.(4.5) and we have from eq.(4.9),

$$X(k,\tau_*) = 1 \quad \text{and} \quad Y(k,\tau_*) = \frac{1}{3} \quad .$$

Notice that $X(k,\tau_0) > 0$ for $\tau_0 \to \tau_*$ as we see from eq.(4.9). Our numerical calculations show that $X(k,\tau_0) > 0$ **for all** τ_0 and k.

B. The primordial power spectrum, Scalar curvature fluctuations and the CMB+LSS data.

The power spectrum of curvature perturbations $\mathcal{R}$ is given by the expectation value $< \mathcal{R}^2 >$ in the state with general initial conditions [2]

$$< \mathcal{R}^2(\vec{x},\eta) > = \left(\frac{m}{M_{PL}} \right)^2 \int_0^\infty \frac{|S_{\mathcal{R}}(k;\eta)|^2}{z^2(\eta)}\ \frac{k^2\,dk}{2\,\pi^2} \ . \tag{4.11}$$

where $z(\eta)$ is given by eq.(2.25). Notice in eq.(4.11) the factor $(m/M_{PL})^2$ in the physical power spectrum expressed in terms of the dimensionless quantities used here.

The power spectrum at time η is customary defined as the power per unit logarithmic interval in k

$$< \mathcal{R}^2(\vec{x},\eta) > = \int_0^\infty \frac{dk}{k}\ P_{\mathcal{R}}(k,\eta) \ .$$

Therefore, the scalar power for general initial conditions is given by the fluctuations behavior by the end of inflation [2] ,

$$P_{\mathcal{R}}(k) = \left(\frac{m}{M_{PL}} \right)^2 \frac{k^3}{2\,\pi^2} \lim_{\eta \to 0^-} \left| \frac{S_{\mathcal{R}}(k;\eta)}{z(\eta)} \right|^2 \ . \tag{4.12}$$

The mode functions $S_{\mathcal{R}}(k;\eta)$ obey the fluctuations equation (2.24) where the potential $W_{\mathcal{R}}(\eta)$ [eq.(2.27)] during slow-roll and to leading order in $1/N$ takes the simple form [2] ,

$$W_{\mathcal{R}}(\eta) = \frac{2}{\eta^2}\left[1+\frac{3}{2}\left(3\,\epsilon_v - \eta_v\right)\right] = \frac{\nu_{\mathcal{R}}^2 - \frac{1}{4}}{\eta^2} \quad , \quad \nu_{\mathcal{R}} = \frac{3}{2} + 3\,\epsilon_v - \eta_v + \mathcal{O}\left(\frac{1}{N^2}\right) . \tag{4.13}$$

In the slow-roll regime we can consider ϵ_v and η_v [see eq.(2.19)] constants in time in eq.(4.13). During slow-roll, the general solution of eq.(2.24) is then given by

$$S_{\mathcal{R}}(k;\eta) = A_{\mathcal{R}}(k)\; g_{\nu_{\mathcal{R}}}(k;\eta) + B_{\mathcal{R}}(k)\; g^*_{\nu_{\mathcal{R}}}(k;\eta) \; , \tag{4.14}$$

with

$$g_\nu(k;\eta) = \frac{1}{2}\; i^{\nu+\frac{1}{2}}\; \sqrt{-\pi\eta}\; H_\nu^{(1)}(-k\,\eta) \; , \tag{4.15}$$

$A_{\mathcal{R}}(k),\; B_{\mathcal{R}}(k)$ are constants determined by the initial conditions and $H_\nu^{(1)}(z)$ is a Hankel function.

The Wronskian of the solutions $S_{\mathcal{R}},\; S^*_{\mathcal{R}}$ is given by eq.(4.4) and

$$W[g_\nu, g_\nu^*] = i$$

This generically determines that

$$|A_{\mathcal{R}}(k)|^2 - |B_{\mathcal{R}}(k)|^2 = 1 \; . \tag{4.16}$$

For wavevectors deep inside the Hubble radius $|k\,\eta| \gg 1$ the mode functions $g_\nu(k;\eta)$ have the asymptotic behavior

$$g_\nu(k;\eta) \stackrel{\eta\to-\infty}{=} \frac{1}{\sqrt{2\,k}}\; e^{-i\,k\,\eta} \quad , \quad g^*_\nu(k;\eta) \stackrel{\eta\to-\infty}{=} \frac{1}{\sqrt{2k}}\; e^{i\,k\,\eta} \; , \tag{4.17}$$

while for $\eta \to 0^-$, they behave as:

$$g_\nu(k;\eta) \stackrel{\eta\to 0^-}{=} \frac{\Gamma(\nu)}{\sqrt{2\,\pi\,k}}\; \left(\frac{2}{i\,k\,\eta}\right)^{\nu-\frac{1}{2}} \; . \tag{4.18}$$

In particular, in the scale invariant case $\nu = \frac{3}{2}$ which is the leading order in the slow-roll expansion, the mode functions eqs.(4.15) simplify to

$$g_{\frac{3}{2}}(k;\eta) = \frac{e^{-i\,k\,\eta}}{\sqrt{2k}}\left[1 - \frac{i}{k\,\eta}\right] \; . \tag{4.19}$$

As we see from eq.(2.25), $z(\eta)$ obeys eq.(2.24) for $k=0$ and therefore $z(\eta)$ in the slow-roll regime behaves as

$$z(\eta) = \frac{z_0}{(-k_0\,\eta)^{\nu_{\mathcal{R}}-\frac{1}{2}}} \; , \tag{4.20}$$

where z_0 is the value of $z(\eta)$ when the pivot scale k_0 exits the horizon, that is at $\eta = -1/k_0$. Combining this result with the small η limit eq.(4.18) we find from eqs.(4.12) and (4.20),

$$P_{\mathcal{R}}(k) = P^{BD}_{\mathcal{R}}(k)\,[1 + D(k)] \; , \tag{4.21}$$

where we introduced the transfer function for the initial conditions of curvature perturbations:

$$D(k) = 2\,|B_{\mathcal{R}}(k)|^2 - 2\,\mathrm{Re}\left[A_{\mathcal{R}}(k)\; B^*_{\mathcal{R}}(k)\, i^{2\nu_{\mathcal{R}}-3}\right] \; . \tag{4.22}$$

$D(k)$ is obtained imposing BDic at $\tau = \tau_0$ according to eq.(4.7).

Notice as shown in sec. V A that the transfer function $D(k)$ enjoys the properties

$$1 + D(k) \stackrel{k\to 0}{=} \mathcal{O}(k^{n_s+1}) \quad , \quad D(k) \stackrel{k\to\infty}{=} \mathcal{O}\left(\frac{1}{k^2}\right) \; . \tag{4.23}$$

$D(k)$ accounts for the effect in the power spectrum both of the initial conditions and of the fluctuations evolution during fast-roll (before slow-roll). $D(k)$ depends on the time τ_0 at which BDic are imposed.

If one chooses the extreme slow-roll solution presented in sec. III A and imposes BDic at $\tau_0 = -\infty$ (that is, $\eta_0 = -\infty$) then $D(k) = 0$ and the fluctuation power spectrum at the end of inflation is the usual power spectrum $P_{\mathcal{R}}(k) = P_{\mathcal{R}}^{BD}(k)$.

$P_{\mathcal{R}}^{BD}(k)$ is given by its customary slow-roll expression,

$$\log P_{\mathcal{R}}^{BD}(k) = \log A_s(k_0) + (n_s - 1)\ \log \frac{k}{k_0} + \tfrac{1}{2}\, n_{run}\ \log^2 \frac{k}{k_0} + \mathcal{O}\left(\frac{1}{N^3}\right)\ . \tag{4.24}$$

We solved numerically the fluctuations equation (2.26) in cosmic time with the BDic eq.(4.7) covering both the fast-roll and slow-roll regimes. We started at initial times τ_0 ranging from the vicinity of $\tau = \tau_*$ till the transition time $\tau_{trans} = 0.2487963\ldots$ from fast-roll to slow-roll. We computed the transfer function $D(k)$ from the mode functions behaviour deep during slow-roll inflation from eqs.(4.12) and (4.21) [2]. In figs. 6 we depict $1 + D(k)$ vs. k for twelve values of the time τ_0 where BDic are imposed.

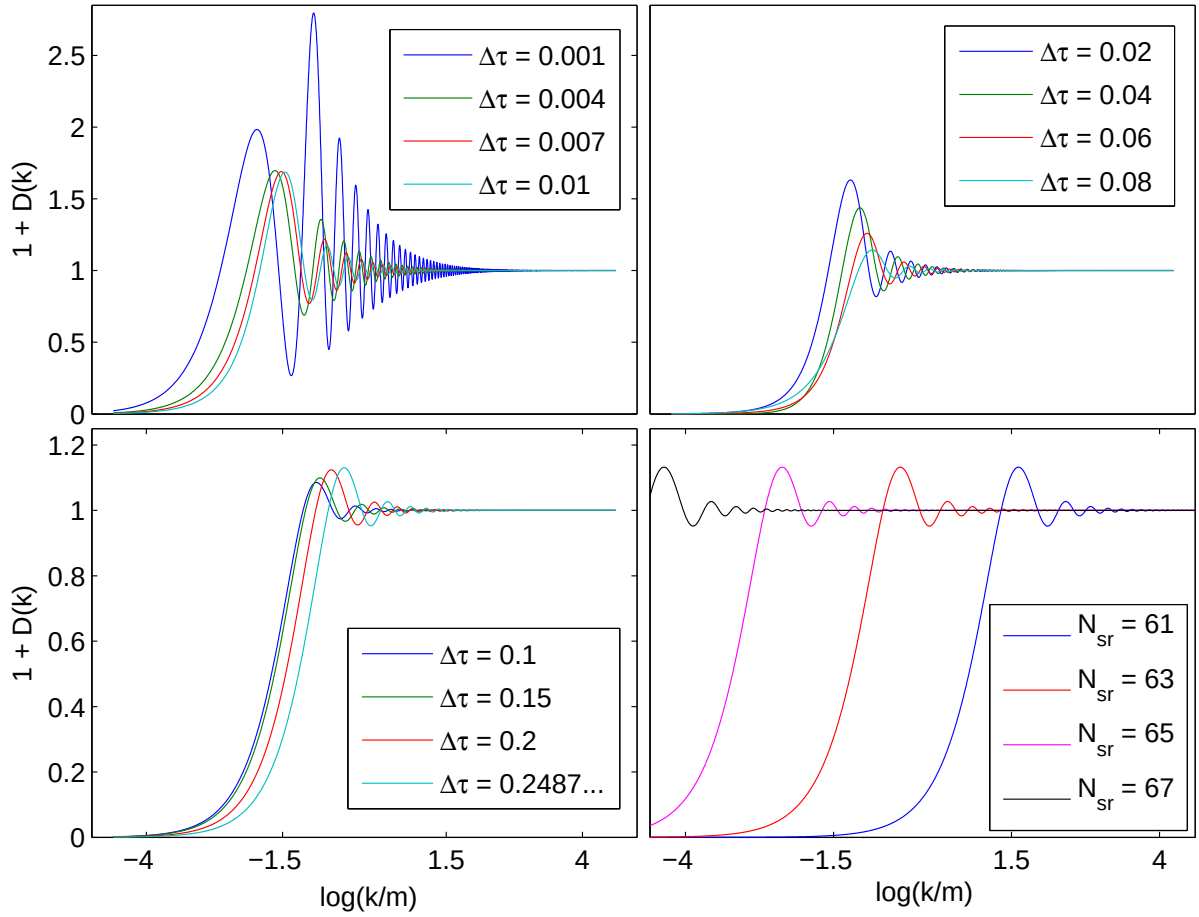

FIG. 6: Numerical transfer function $1 + D(k)$. Lower left panel: Numerical transfer function $1 + D(k)$ for BDic at $\tau = \tau_0 = \tau_* + \Delta\tau$, for different $\Delta\tau$ values as given in the picture. We see here that the peak of $1 + D(k)$ grows and moves for larger k as τ_0 increases. Here $N_{sr} = 63$. Lower right panel: The transfer function $1 + D(k)$ when the BDic eq.(4.7) are imposed during slow–roll at finite times τ_0 and N_{sr} efolds of slow–roll have still to occur. Upper panels: Numerical transfer function $1 + D(k)$ for BDic at $\tau = \tau_0 = \tau_* + \Delta\tau$, for different values of $\Delta\tau$ as given in the picture. We get stronger oscillations in $1 + D(k)$ for decreasing τ_0 in the range $\Delta\tau < 0.04$. Here $N_{sr} = 63$.

Notice that when BDic are imposed at **finite times** τ_0, the spectrum **is not** the usual $P_{\mathcal{R}}^{BD}(k)$ but it gets modified by a non-zero transfer function $D(k)$ eq.(4.21). The power spectrum $P_{\mathcal{R}}(k)$ vanishes at $k = 0$ and exhibits oscillations which vanish at large k [see figs. 6 and 7].

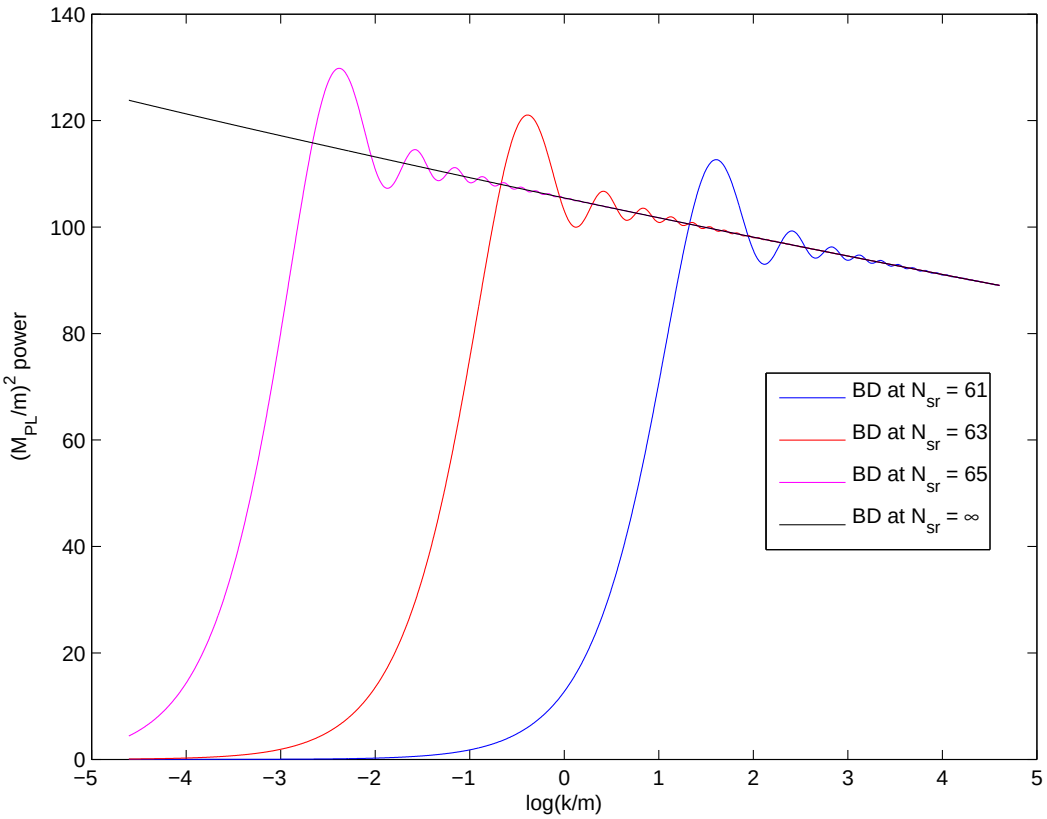

FIG. 7: Power spectrum with BDic eq.(4.7) imposed during slow–roll when N_{sr} efolds of slow–roll inflation have still to occur. We see here the decrease of the power spectrum $P_{\mathcal{R}}$ as k^{n_s-1} multiplied by the oscillations of $1+D(k)$. See eqs.(4.21) and (4.24) and figs. 6. The non-oscillatory black curve corresponds to the usual power with BDic at $\eta_0=-\infty$ eq.(4.24) decreasing as k^{n_s-1}. The later are imposed the BDic, the smaller is the number of slow-roll efolds N_{sr} and the whole k-spectrum shifts to larger k.

During slow-roll different initial times τ_0 lead essentially to a rescaling of k in $D(k)$ by a factor η_0 since the conformal time η is almost proportional to $1/a(\eta)$ during slow-roll [see figs. 7- 6 and below eq.(5.7)]. By virtue of the dynamical attractor character of slow–roll, the power spectrum when the BDic are imposed at a finite time τ_0 cannot really distinguish between the extreme slow–roll solution (for which slow–roll starts from the very beginning $\eta_0=-\infty$) or any other solution which is attracted to slow–roll well before the time τ_0.

C. Accurate numerical computation of the power spectrum and the transfer function $D(k)$ of initial conditions.

In order to accurately calculate n_s we proceed as follow. We match the solution $S_{\mathcal{R}}(k;\eta)$ with the slow–roll solution $g_{\nu_{\mathcal{R}}}(k;\eta)$ eq.(4.15) at the time τ_0 when N_{sr} efolds of slow–roll have still to occur. η and $\nu_{\mathcal{R}}$ are computed at this time τ_0. In practice, this corresponds to setting $A_{\mathcal{R}}(k)=1$, $B_{\mathcal{R}}(k)=0$ (and therefore $D_{\mathcal{R}}(k)=0$) in the Bogoliubov transformation eq.(4.14).

Then, we integrate numerically the fluctuations equations eq.(2.26). By construction, this produces the standard spectra $P_{\mathcal{R}}^{BD}(k)$ eq.(4.24) that quickly stabilize as N_{sr} is increased a few efolds above $N=60$.

It is convenient to introduce the quantity

$$L_s \equiv \log\left[\left(\frac{M_{PL}}{m}\right)^2 A_s(k_0=m)\right] , \tag{4.25}$$

with $k_0=m$ when $a(\eta)=1$, that is $N=60$ efolds before inflation ends. In table IV we provide L_s for several values of N_{sr}.

N_{sr}	L_s	n_s	n_{run}
61	$4.6585381\ldots$	$0.9637013\ldots$	$-0.0000701\ldots$
63	$4.6583004\ldots$	$0.9641135\ldots$	$-0.0001639\ldots$
65	$4.6584371\ldots$	$0.9642483\ldots$	$-0.0002165\ldots$
67	$4.6584463\ldots$	$0.9642444\ldots$	$-0.0002165\ldots$
69	$4.6584469\ldots$	$0.9642448\ldots$	$-0.0002167\ldots$

TABLE IV: Exact values of $L_s = \log[(M_{PL}/m)^2\ A_s(k_0 = m)]$ for several values of N_{sr} from the numerical calculation. The exact values of n_s vary little with N_{sr} and are close to the slow-roll approximation value. Also n_{run} is close to the value in the slow-roll approximation.

To transform this k_0 in a wavenumber today we need:

- the total redshift from 60 efolds before inflation ends till today [since we choose $a(\tau = 0) = 1$ when there are still $N = 60$ efolds till the end of inflation].
- the value of m as determined by the observed value of the amplitude $A_s(k_0)$.

Let $k_0^{\rm CMC}$ be the value of the pivot scale of CosmoMC [that is 50 $({\rm Gpc})^{-1}$ today] 60 efolds before the end of inflation. Then, we have from eqs.(4.24) and (4.25),

$$\log A_s(k_0 = m) = L_s + 2\,\log\frac{m}{M_{PL}} = L_s^{\rm CMC} + (n_s^{\rm CMC} - 1)\ \log\frac{m}{k_0^{\rm CMC}} + \tfrac{1}{2}\ n_{run}\ \left[\log\frac{m}{k_0^{\rm CMC}}\right]^2 + \mathcal{O}\left(\frac{1}{N^3}\right)\ , \quad (4.26)$$

where $L_s^{\rm CMC} \equiv \log A_s^{\rm CMC}(k_0^{\rm CMC})$ and $n_s^{\rm CMC}$ are best fit values in a given CosmoMC run. Since the running index n_{run} is $\mathcal{O}\left(1/N^2\right)$, we get for m,

$$\left(\frac{m}{M_{PL}}\right)^2 = \left(\frac{m}{k_0^{\rm CMC}}\right)^{n_s^{\rm CMC}-1} \exp\left(L_s^{\rm CMC} - L_s\right)\left[1 + \mathcal{O}\left(\frac{1}{N^2}\right)\right]\ . \quad (4.27)$$

The wavevectors at $a = 1$ (60 efolds before inflation ends) and today are related by [2]

$$k^{a=1} = \frac{e^{60}}{a_r}\ k^{today}\ , \quad (4.28)$$

where a_r is the scale factor by the end of inflation

$$a_r = 2.5\ 10^{-29}\ \sqrt{\frac{10^{-4} M_{PL}}{H_{60}}}\ , \quad (4.29)$$

and H_{60} is the Hubble parameter 60 efolds before inflation ends. We thus have for the pivot wavenumber at $a = 1$

$$k_0^{\rm CMC} \simeq 1.46\ldots\ \sqrt{\frac{H_{60}}{10^{-4} M_{PL}}} \times 10^{15}\ {\rm GeV} \quad (4.30)$$

and

$$\left(\frac{m}{M_{PL}}\right)^{2-(n_s^{\rm CMC}-1)/2} = \left(\frac{16.67\ldots}{\sqrt{h_{60}}}\right)^{n_s^{\rm CMC}-1} \exp\left(L_s^{\rm CMC} - L_s\right) \quad , \quad \text{where} \quad h_{60} \equiv \frac{H_{60}}{m}\ .$$

Notice the small $1/N$ correction $(n_s^{\rm CMC} - 1)/2$ in the exponent of m/M_{PL}. Eq.(4.26) yields for the best fit CosmoMC run $L_s^{\rm CMC} = -19.9808\ldots$ and $n_s = 0.9635\ldots$ [2]:

$$m \simeq 4.8114\ldots 10^{-6}\, M_{PL} = 1.1717\ldots 10^{13}\ {\rm GeV}$$

The exact values given above in Table IV

$$A_s = \left(\frac{m}{M_{PL}}\right)^2\ \exp(L_s)\ , \quad n_s \quad \text{and} \quad n_{run}$$

are obtained taking into account the fast-roll and slow–roll stages in the numerical calculation. We can compare them to their slow–roll (leading $1/N$) analytic counterparts for the double-well quadratic plus quartic potential, [2]

$$A_s = \frac{N^2}{12\pi^2}\left(\frac{m}{M_{PL}}\right)^2 \frac{(1-z)^4}{y^2\,z}\,, \quad n_s = 1 - \frac{y}{N}\,\frac{3\,z+1}{(1-z)^2}\,, \quad n_{run} = \frac{y^2\,z}{N^2\,(1-z)^4}\left(24\,z^2 - 35\,z + 3\right)$$

where $N = 60,\ z = 0.117446$ and $y = z - 1 - \log z = 1.2592226\ldots$, that is

$$A_s = \frac{N^2}{12\pi^2}\,\left(\frac{m}{M_{PL}}\right)^2 \exp(4.59536898\ldots)\,, \quad n_s = 0.9635620\ldots\,, \quad n_{run} = -0.0000664\ldots$$

The figure in the exponent is to be compared with the L_s values in Table IV. The agreement with Table IV is quite good, especially for n_s.

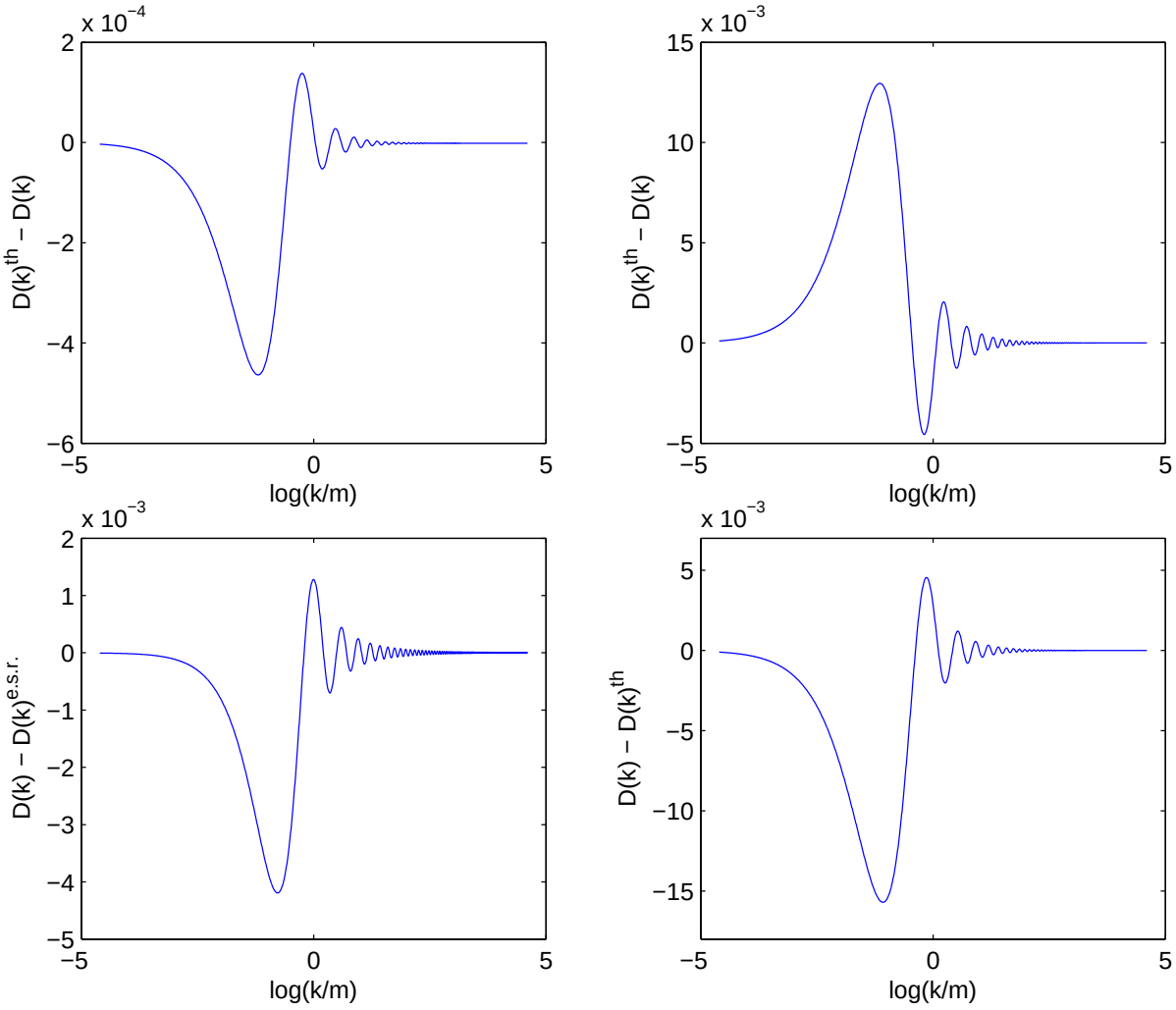

FIG. 8: Upper Left panel: Difference between the (approximate) transfer function $\tilde{D}(k\,\eta_0)$ eqs.(5.7)-(5.9) for $\nu_{\mathcal{R}} = 1.5182189\ldots$ and the numerical (exact at least to a 10^{-7} relative error) transfer function $D(k)$, when $N_{sr} = 63$. Upper Right panel: Difference between the (approximate) transfer function $\tilde{D}(k\,\eta_0)$ eqs.(5.7)-(5.9) for $\nu_{\mathcal{R}} = 3/2$ (the scale-invariant value) and the numerical (exact) transfer function. We see that the difference in the right panel [eq.(5.9)] is < 0.014 while in the left panel the difference of the analytic formula eq.(5.7) is much smaller, < 0.0005. Lower Left panel: difference between the exact (numerical) $D(k)$ computed for the fast-roll inflaton solution of table II and for the extreme slow–roll inflaton solution of table I when BDic are imposed 63 efolds before the end of inflation. Lower Right panel: difference between the numerical (exact) fast–roll $D(k)$ and the approximate $\tilde{D}(k\,\eta_0)$ calculated with $\nu_{\mathcal{R}} = 3/2$ and $\eta_0 = -4.0169827\ldots$. We see that the differences are small in both cases.

We now find the exact (numerical) transfer function $D(k)$ for the initial conditions, by simply taking in eq.(4.21) the ratio of the two power spectra: $P_{\mathcal{R}}(k)$ with BDic at time τ_0 and $P_{\mathcal{R}}^{BD}(k)$. In the case of BDic at finite times the result is given in fig 6. At the largest value $k/m = 100$ of the wavenumber interval considered, we have

$$1 + D(100\, m) = 0.9996994\ldots,\ 1.0000061\ldots,\ 1.0000001\ldots$$

for

$$N_{sr} = 61,\ 63,\ 65 \text{ and } 67, \text{ respectively.}$$

This provides a good check of the accuracy of the calculation.

In figs. 8 we compare the numerically computed $D(k)$ against $\tilde{D}(k\,\eta_0)$ analytically computed for BDic imposed at time η_0 during slow–roll in eq.(5.7), sec. V B. The comparison is performed for BDic imposed when $N_{sr} = 63$ on the extreme slow roll solution, which corresponds to $\eta_0 = -4.0202308\ldots$. We consider two values of $\nu_{\mathcal{R}}$: $\nu_{\mathcal{R}} = 2 - n_s/2 = 1.5182189\ldots$, $n_s = 0.9635620\ldots$ corresponding to slow–roll at leading $1/N$ order, and the exactly scale-invariant case $\nu_{\mathcal{R}} = 3/2$. Notice that in the latter case $\tilde{D}(k\,\eta_0)$ has the explicit simple analytic form eq.(5.9).

The maximum of the numerical transfer function $1 + D(k)$ is located at $k/m = 0.68755\ldots$ and has the value $1.13218\ldots$ The maximum of $1 + \tilde{D}(k\,\eta_0)$, when $\nu_{\mathcal{R}} = 3/2$ is in $k/m = 0.68755\ldots$ and has the value $1.13009\ldots$. Recall that these values of k/m have the scale fixed by the choice $a = 1$ when $N = 60$ efolds lack before inflation ends.

Let us now consider the fluctuations on the fast–roll solution of Table II. Since η has a finite lower limit, the choice $A_{\mathcal{R}}(k) = 1,\ B_{\mathcal{R}}(k) = 0$ has little meaning and BDic can be imposed only at a finite time τ_0 later than the singularity time τ_*. If τ_0 is exactly the transition time τ_{trans} when $\epsilon_v = 1/N$, fast-roll ends and slow–roll begins, (to proceed for $N_{sr} = 63$ efolds), then $D(k)$ does not differ too much from that computed with the extreme slow roll solution. This comparison is performed in the lower left panel of fig. 8. In the right panel $D(k)$ is compared to the $\tilde{D}(k\,\eta_0)$ for $\nu_{\mathcal{R}} = 3/2$ and $\eta_0 = -4.0169827\ldots$, which is the value of the conformal time at the onset of slow–roll (see Table II).

When the BDic are imposed during the fast–roll stage well **before** it ends, $D(k)$ changes much more significantly than along the extreme slow roll solution. This is due to two main effects: the potential felt by the fluctuations is attractive during fast–roll and η_0, far from being almost proportional to $1/a(\eta)$, tend to the constant value η_* as $\tau \to \tau_*^+$ and $a(\eta) \to 0$. The numerical transfer functions $1 + D(k)$ obtained from eqs.(4.12) and (4.21) are plotted in figs. 6.

The fact that choosing BDic leads to a primordial power and its respective CMB multipoles which correctly **reproduce** the observed spectrum justifies the use of BDic for the scalar curvature fluctuations.

D. The effect of the fast-roll stage on the low multipoles of the CMB

In the region of the Sachs-Wolfe plateau for $l \lesssim 30$, the matter-radiation transfer function can be set equal to unity and the CMB multipole coefficients $C_l's$ are given by [9]

$$C_l = \frac{4\pi}{9} \int_0^\infty \frac{dk}{k}\, P_X(k)\, \{j_l[k(\eta_0 - \eta_{LSS})]\}^2\ , \tag{4.31}$$

where P_X is the power spectrum of the corresponding perturbation, $X = \mathcal{R}$ for curvature perturbations and $X = T$ for tensor perturbations, $j_l(x)$ are spherical Bessel functions [8] and $\eta_0 - \eta_{LSS}$ is the comoving distance between today and the last scattering surface (LSS) given by

$$\eta_0 - \eta_{LSS} = \frac{1}{H_0} \int_{\frac{1}{1+z_{LSS}}}^1 \frac{da}{\sqrt{\Omega_r + \Omega_M\, a + \Omega_\Lambda\, a^4}}\ , \tag{4.32}$$

where Ω_r, Ω_M and Ω_Λ stand for the fraction of radiation, matter and cosmological constant in today's Universe. We find using $z_{LSS} = 1100$,

$$\eta_0 - \eta_{LSS} = \frac{3.296}{H_0}\ . \tag{4.33}$$

Notice that $k/H_0 \sim d_H/\lambda_{phys}(t_0)$ is the ratio between today's Hubble radius and the physical wavelength. The power spectrum for curvature ($\mathcal{R}$) perturbations $P_{\mathcal{R}}(k)$ is given by eqs.(4.21)-(4.24).

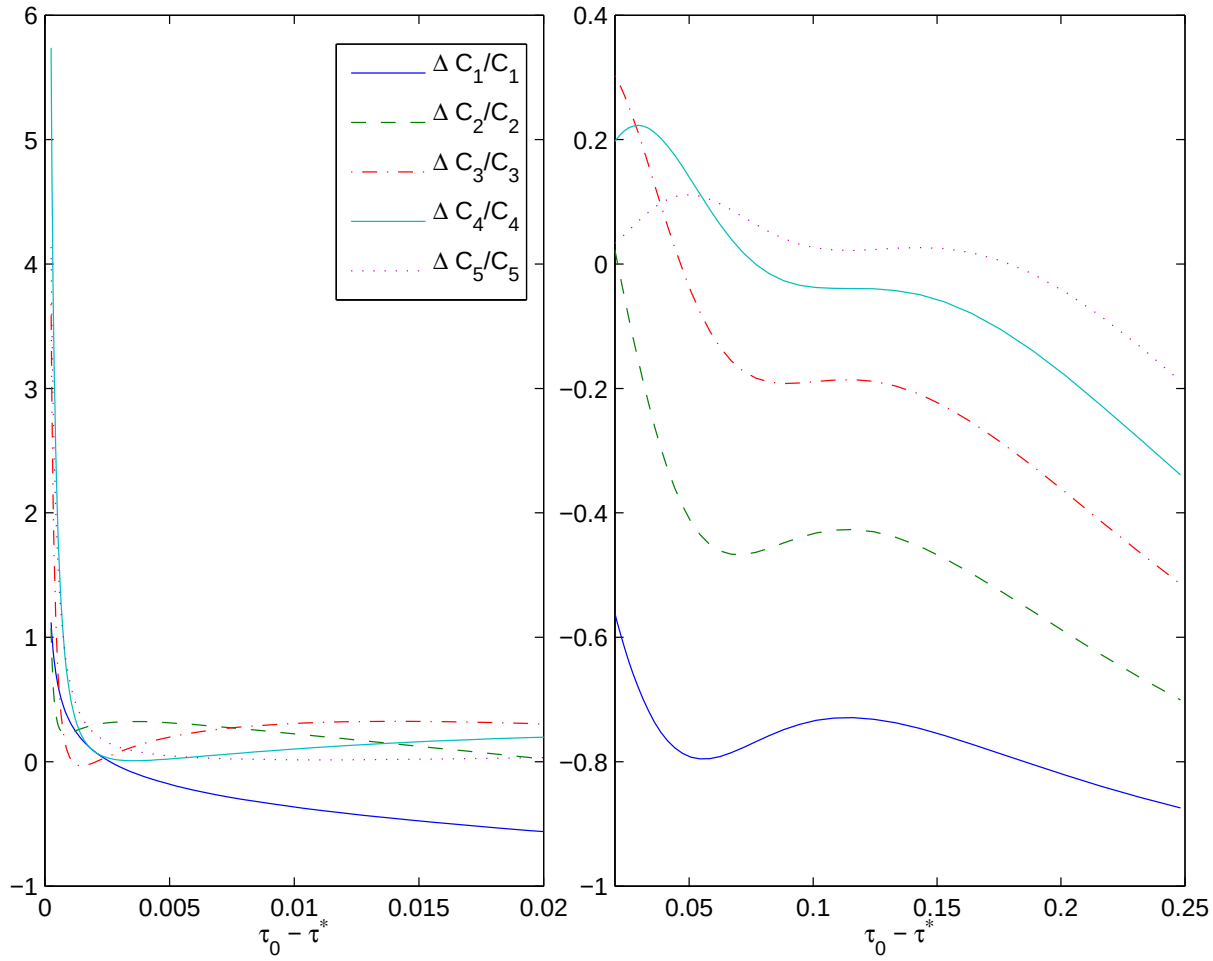

FIG. 9: The change $\Delta C_\ell/C_\ell$ on the CMB multipoles for $\ell = 1, \ldots, 5$. Upper plot: $\Delta C_\ell/C_\ell$ vs. $\tau_0 - \tau_*$ for $0 < \tau_0 - \tau_* < 0.2487963\ldots$. Lower plot: $\Delta C_\ell/C_\ell$ vs. $\tau_0 - \tau_*$ for $0.0193 < \tau_0 - \tau_* < 0.2487963\ldots$. τ_0 is the time when the BDic eq.(4.7) are imposed to the fluctuations. We choose τ_0 inside the fast-roll stage. $\Delta C_\ell/C_\ell$ is **positive** for small $\tau_0 - \tau_*$ and **decreases** with τ_0 becoming then **negative**. The CMB quadrupole observations indicate a large **suppression** thus indicating that $\tau_0 - \tau_* \gtrsim 0.05 \simeq 10100\ \tau_{Planck}$. Our **predictions** here for the quadrupole and octupole suppressions are to be confronted with forthcoming CMB observations. It will be extremely interesting to measure the primordial dipole and compare with our predicted value.

Inserting eq.(4.21) into eq.(4.31) yields the C_l as the sum of two terms

$$C_l = C_l^{BD} + \Delta C_l \quad , \quad \frac{\Delta C_l}{C_l} = \frac{\int_0^\infty D(\kappa\, x)\ f_l(x)\ dx}{\int_0^\infty f_l(x)\ dx} \quad , \quad x = k(\eta_0 - \eta_{LSS}) = k/\kappa\ , \tag{4.34}$$

where from eq.(4.33), $\kappa \equiv H_0/3.296\ldots$,

$$f_l(x) = x^{n_s - 2}\ [j_l(x)]^2\ . \tag{4.35}$$

and $j_l(x)$ stand for the spherical Bessel functions.

The C_l^{BD}'s correspond to the standard BD power spectrum $P_{\mathcal{R}}^{BD}(k)$ eq.(4.24) and the ΔC_l exhibit the effect of the transfer function $D(k)$ on the C_l.

Using the transfer function $D(k)$ obtained above eq.(4.22), we computed the change on the CMB multipoles $\Delta C_\ell/C_\ell$ for $\ell = 1, \ldots, 5$ as functions of the starting instant of the fluctuations τ_0. We plot $\Delta C_\ell/C_\ell$ for $1 \leq \ell \leq 5$ vs. $\tau_0 - \tau_*$ in fig. 9. We see that $\Delta C_\ell/C_\ell$ is **positive** for small $\tau_0 - \tau_*$ and **decreases** with τ_0 becoming then **negative**. The CMB quadrupole observations indicate a large **suppression** thus indicating that $\tau_0 - \tau_* \gtrsim 0.05 \simeq 10100\ \tau_{Planck}$.

Being $D(k) < 0$ for low k as depicted in figs. 6, the primordial power at large scales is then suppresed and the low C_ℓ decrease as seen from eq.(4.34).

$\Delta C_\ell/C_\ell$ mainly originates from the peak of $D(k)$ displayed in figs. 6 whose position moves to smaller k for decreasing τ_0. Therefore, the primordial power suppression is less important for decreasing τ_0 and the CMB multipole suppression $\Delta C_\ell/C_\ell$ less important as depicted in figs. 9.

For small $\tau_0 - \tau_* \lesssim 0.05$ the peak of $D(k)$ grows significantly and $\Delta C_\ell/C_\ell$ become positive, namely the low CMB multipoles are enhanced.

It should be recalled that the observation of a low CMB quadrupole sparked many different proposals to explanain that suppression [18].

Besides finding a CMB quadrupole suppression in agreement with observations [2]-[6], we provide here **predictions** for the dipole and octupole suppressions. Forthcoming CMB observations can provide better data to confront our quadrupole and octupole suppression predictions. It will be extremely interesting to measure the primordial dipole and compare with our predicted value.

V. ANALYTIC FORMULAS FOR THE TRANSFER FUNCTION $D(k)$.

It is very important to dispose of analytic formulas for the transfer function $D(k)$ in order to better understand the physical origin of its oscillations and properties as well as in the perspective of the MCMC data analysis.

However, the mode equations (2.24) are not solvable in closed form for $k \neq 0$, not even for the approximated inflation solution eq.(2.37) which leads to the potential $V_{\mathcal{R}}(\tau)$ eq.(2.43).

The function $D(k)$ must obey the general properties eq.(4.23).

A. The primordial power spectrum vanishes for $k \to 0$ and becomes the BD power spectrum for $k \to \infty$

The fluctuations equation (2.24) can be solved explicitly for $k = 0$

$$s(\eta) = c_1\ z(\eta) + c_2\ z(\eta)\ \int_{\eta_0}^{\eta} \frac{d\eta'}{z^2(\eta')}\ , \tag{5.1}$$

where c_1 and c_2 are arbitrary constants.

The BDic eq.(4.7) introduce for $k \to 0$ a $1/\sqrt{2\,k}$ singularity in the mode functions. Thus, the mode functions must have the behaviour

$$S_{\mathcal{R}}(k;\eta) \stackrel{k\to 0}{=} \frac{s(\eta)}{\sqrt{2\,k}}\,[1 + \mathcal{O}(k)] \tag{5.2}$$

where $s(\eta)$ is given by eq.(5.1).

Inserting eq.(5.2) into the BDic eq.(4.7) yields for $k \to 0$,

$$s(\eta_0) = 1 \quad , \quad \frac{ds(\eta_0)}{d\eta} = 0\ ,$$

which determines the coefficients c_1 and c_2 in eq.(5.1). We finally obtain

$$s(\eta) = \frac{z(\eta)}{z(\eta_0)} - z'(\eta_0)\ z(\eta)\ \int_{\eta_0}^{\eta} \frac{d\eta'}{z^2(\eta')} \tag{5.3}$$

and using eq.(4.20) valid for $\eta \to 0^-$ when slow–roll applies

$$\lim_{\eta\to 0^-} \frac{s(\eta)}{z(\eta)} = \frac{1}{z(\eta_0)}\ . \tag{5.4}$$

The primordial power spectrum for $k \to 0$ follows by inserting eq.(5.2) and eq.(5.4) into the general expression eq.(4.12),

$$P_{\mathcal{R}}(k) \stackrel{k\to 0}{=} \left(\frac{m}{M_{PL}}\right)^2\ \frac{k^3}{2\,\pi^2}\ \lim_{\eta\to 0^-}\left|\frac{S_{\mathcal{R}}(k;\eta)}{z(\eta)}\right|^2 \stackrel{k\to 0}{=} \left(\frac{m}{M_{PL}}\right)^2\ \left(\frac{k}{2\,\pi\ z(\eta_0)}\right)^2$$

We thus find in general that the power spectrum vanishes as k^2 for $k \to 0$ and therefore

$$1 + D(k) \stackrel{k\to 0}{=} \mathcal{O}(k^{n_s+1})$$

as stated in eq.(4.23). This property is generally true except for the extreme slow-roll inflaton solution (sec. III A) with BDic imposed at $\eta_0 = -\infty$ in which case $D(k)$ vanishes identically for all k.

For growing k the modes exit the horizon later on, during the slow–roll regime where eq.(4.14) applies. For large k the mode functions $S_{\mathcal{R}}$ as well as $g_{\nu_{\mathcal{R}}}$ behave as plane waves [eqs.(4.6) and (4.18)] and therefore

$$A_{\mathcal{R}}(k) = 1 \quad , \quad B_{\mathcal{R}}(k) = 0 \quad . \quad \text{Hence} \quad D(k) \stackrel{k\to\infty}{=} 0 \; .$$

.

B. The transfer function $D(k)$ when BDic are imposed during slow–roll.

When the BDic eq.(4.7) are imposed during slow–roll at a finite time η_0 we can use eq.(4.14) for the mode functions at $\eta = \eta_0$ and we obtain,

$$\begin{aligned} \frac{e^{-i\,k\,\eta_0}}{\sqrt{2\,k}} &= A_{\mathcal{R}}(k)\; g_{\nu_{\mathcal{R}}}(k;\eta_0) + B_{\mathcal{R}}(k)\; g^*_{\nu_{\mathcal{R}}}(k;\eta_0) \\ -i\,k\,\frac{e^{-i\,k\,\eta_0}}{\sqrt{2\,k}} &= A_{\mathcal{R}}(k)\; g'_{\nu_{\mathcal{R}}}(k;\eta_0) + B_{\mathcal{R}}(k)\; g'^*_{\nu_{\mathcal{R}}}(k;\eta_0) \end{aligned} \tag{5.5}$$

which determines

$$A_{\mathcal{R}}(k) = \frac{e^{-i\,k\,\eta_0}}{i\,\sqrt{2\,k}}\left[g'^*_{\nu_{\mathcal{R}}}(k;\eta_0) + i\,k\; g^*_{\nu_{\mathcal{R}}}(k;\eta_0)\right] \quad , \quad B_{\mathcal{R}}(k) = \frac{e^{-i\,k\,\eta_0}}{i\,\sqrt{2\,k}}\left[g'_{\nu_{\mathcal{R}}}(k;\eta_0) + i\,k\; g_{\nu_{\mathcal{R}}}(k;\eta_0)\right] \; . \tag{5.6}$$

These coefficients satisfy eq.(4.16) and

$$|A_{\mathcal{R}}(k)|^2 + |B_{\mathcal{R}}(k)|^2 = \frac{1}{k}\left[|g'_{\nu_{\mathcal{R}}}(k;\eta_0)|^2 + k^2\;|g_{\nu_{\mathcal{R}}}(k;\eta_0)|^2\right]$$

Notice that the function $g_\nu(k;\eta)$ eq.(4.15) and the k factors in eq.(5.6) combine to produce functions $A_{\mathcal{R}}(k) \equiv \tilde{A}_{\mathcal{R}}(k\;\eta_0)$ and $B_{\mathcal{R}}(k) \equiv \tilde{B}_{\mathcal{R}}(k\;\eta_0)$ that only depend on the product $k\;\eta_0$.

We find from eqs.(4.22) and (5.6) the corresponding transfer function which is a function of $k\;\eta_0$ too,

$$1 + \tilde{D}(k\;\eta_0) = \frac{1}{k}\left\{|g'_{\nu_{\mathcal{R}}}(k;\eta_0)|^2 + k^2\;|g_{\nu_{\mathcal{R}}}(k;\eta_0)|^2 - \mathrm{Re}\left[i^{3-2\,\nu_{\mathcal{R}}}\;\left(g'^2_{\nu_{\mathcal{R}}}(k;\eta_0) + k^2\;g^2_{\nu_{\mathcal{R}}}(k;\eta_0)\right)\right]\right\} \tag{5.7}$$

The functional dependence on $k\;\eta_0$ confirms the assertion in sec. IV B that different initial times τ_0 lead to a rescaling in k.

In the $k\;\eta_0 \to \infty$ limit two types of vanishing terms show up in $\tilde{D}(k\;\eta_0)$: (a) terms that strongly oscillate as $e^{\pm 2\,i\,k\,\eta_0}$ as they tend to zero and (b) non-oscillatory decreasing terms. Under integrals on k, the terms of type (a) yield convergent expressions. We derive the non-oscillatory decreasing terms (b) by inserting the asymptotic behaviour of the Hankel functions eq.(4.15) [8] in eq.(5.7) with the result

$$\tilde{D}(k\;\eta_0) \stackrel{k\to\infty}{=} \frac{(\nu^2 - \frac{1}{4})^2}{8\;(k\;\eta_0)^4} + \text{terms oscillating as } e^{\pm 2\,i\,k\,\eta_0} \; . \tag{5.8}$$

However, this approximation will not be valid for large enough k since the modes at small enough wavelength will exit the horizon after the end of slow–roll where eq.(5.8) does not apply anymore. We recall that the occupation number $|B_{\mathcal{R}}(k)|^2$ (and therefore $D(k)$) must decrease faster than $1/k^4$ for $k \to \infty$ in order to ensure finite UV values for the expectation value of the energy-momentum fluctuations [2, 13].

The case $\nu_{\mathcal{R}} = 3/2$ is a good approximation which simplifies the expressions above. We obtain in this scale invariant case:

$$A_{\mathcal{R}}(k) = 1 + \frac{i}{k\;\eta_0} - \frac{1}{2\;k^2\;\eta_0^2} \quad , \quad B_{\mathcal{R}}(k) = -\frac{e^{-2\,i\,k\,\eta_0}}{2\;k^2\;\eta_0^2} \; .$$

The transfer function is in this case,

$$\tilde{D}(x) = \frac{\cos 2x}{x^2} - \frac{\sin 2x}{x^3} + \frac{\sin^2 x}{x^4} \quad , \quad \nu_{\mathcal{R}} = 3/2 \quad , \quad x \equiv k\, \eta_0 \, . \tag{5.9}$$

Eq.(5.8) for $\nu = 3/2$ coincides with eq.(5.9) in the $x \to \infty$ limit, as it must be.

Notice that the simple formula eq.(5.9) obeys the general properties eq.(4.23). In particular,

$$\tilde{D}(x) \stackrel{x \to 0}{=} -1 + \frac{4}{9}\, x^2 + \mathcal{O}(x^4) \, .$$

VI. FIXING THE TOTAL NUMBER OF INFLATION E-FOLDS AND THE BOUND FROM ENTROPY

It is very useful to plot the comoving scales of the cosmological fluctuation wavenumbers and the comoving Hubble radius together [see fig. 10]. One sees in this way how and when the cosmological fluctuations cross out and in the Hubble radius. The comoving Hubble radius is defined by $R_H \equiv 1/[a(\tau)\ H(\tau)]$. We display in Table VI the dependence of R_H on the scale factor a for all the relevant eras of the universe.

Expansion stage	Dependence of R_H on a
Extreme Fast-roll	a^2
Fast-roll	$a^2/\sqrt{a^6 + \text{constant}}$
Slow–Roll inflation	$1/a$
Radiation Dominated	a
Matter Dominated	$\sqrt{a}$

TABLE V: Dependence of the comoving Hubble radius $R_H = 1/[a\ H]$ on the scale factor a for the relevant eras of the universe.

The observed CMB quadrupole suppression can be easily explained if it exited the horizon by the end of fast-roll [5, 6]. In that case, the modes which are horizon size today had wavenumbers $k_Q \simeq 11.5\ m$ at horizon exit [6]. Combining this value of k_Q with the redshift since the pivot wavenumber exited the horizon, eqs. (4.28), (4.29) and (4.30), determines the total redshift since the beginning of inflation to be

$$z_{tot} = 0.9\ 10^{56} \ \simeq e^{129} \, .$$

Combining this value with the value of $1 + z_r \simeq 4\ 10^{28} \simeq e^{66}$ by the end of inflation eq.(4.29) yields a total number of $N_{tot} = 63$ inflation efolds. This value is very close to the minimal number of inflation efolds required to explain the entropy of the present universe due to photons and neutrinos [2]:

$$N_{tot} \geq 62.4 \, .$$

Namely, this is the minimum number of inflation efolds compatible with the present entropy of the universe.

In summary, assuming that the CMB quadrupole is suppressed because it exited the horizon by the end of fast-roll inflation **fixes** the total number of inflation efolds which turns to be

$$N_{tot} \simeq 63 \, .$$

Acknowledgments

We thank Anthony Lasenby for fruitful discussions and his interest in this work.

[1] E. Komatsu et al.(WMAP collaboration), Astrophys. J. Suppl. 180:330 (2009).
G. Hinshaw et al.(WMAP collaboration), Astrophys. J. Suppl. 180:225 (2009).
M. R. Nolta et al.(WMAP collaboration), Astrophys. J. Suppl. 180:296 (2009).

[2] D. Boyanovsky, C. Destri, H. J. de Vega, N. Sanchez, arXiv:0901.0549, Int. J. Mod. Phys. **A 24**, 3669-3864 (2009).

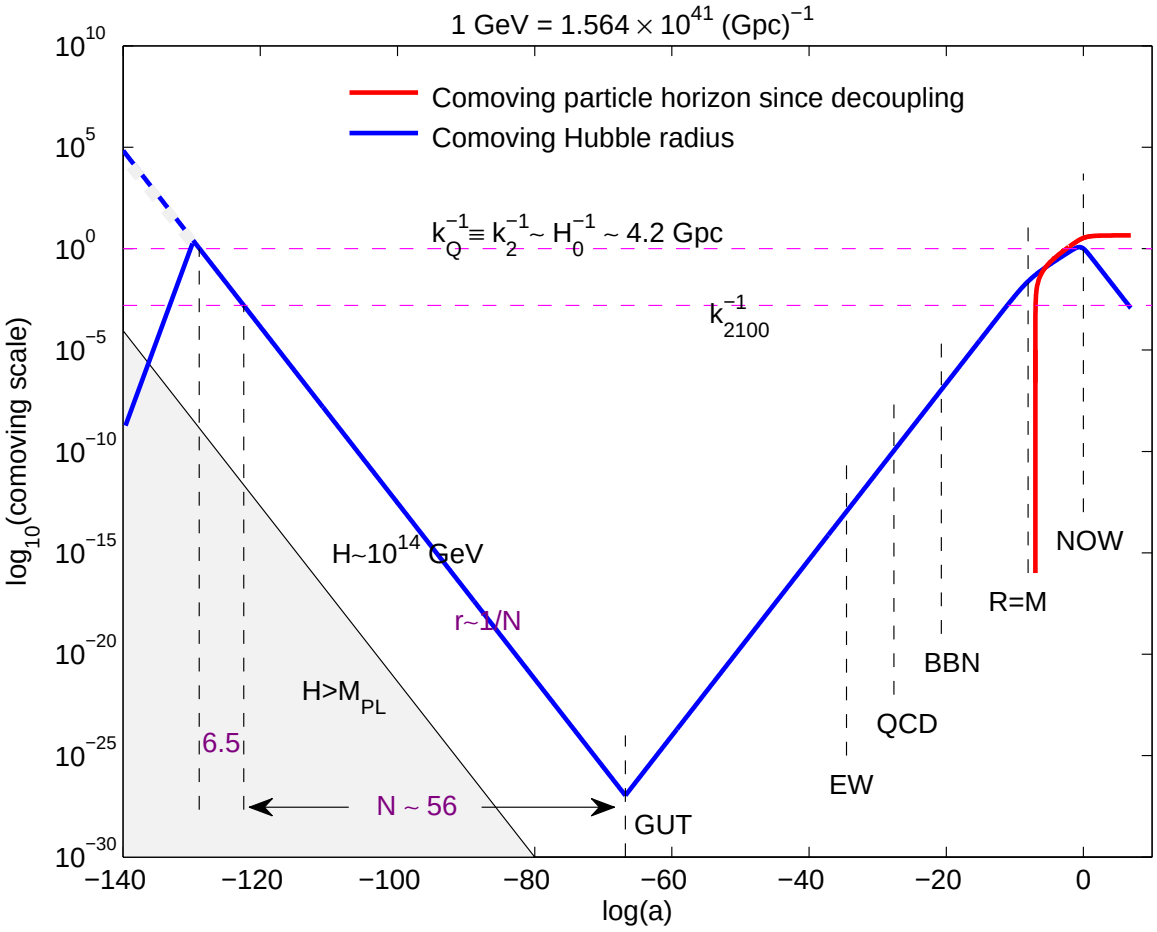

FIG. 10: The logarithm of the comoving scales and the logarithm of the comoving Hubble radius $R_H = 1/[a\ H]$ vs. $\log a$.

[3] L.D. Landau and E.M. Lifshitz, Quantum mechanics, London, Pergamon Press, 1958.

[4] V. A. Belinsky, L. P. Grishchuk, Ya. B. Zeldovich, I. M. Khalatnikov, Phys. Lett. **B 155**, 232, (1985), JETP **62**, 195 (1985).

[5] D. Boyanovsky, H. J. de Vega, N. G. Sánchez, Phys. Rev. **D 74**, 123006 and 123007 (2006).

[6] C. Destri, H. J. de Vega, N. G. Sánchez, Phys. Rev. **D 78**, 023013 (2008).

[7] C. Destri, H. J. de Vega, N. G. Sánchez, Phys. Rev. **D 77**, 043509 (2008).

[8] Handbook of Mathematical Functions, M. Abramowitz and I. A. Stegun, NBS, Washington, 1970.

[9] See for example: Hu W., Dodelson S., *Ann. Rev. Astron. Ap.* 40: 171 (2002); Lidsey J, Liddle A, Kolb E, Copeland E, Barreiro T, Abney M, *Rev. of Mod. Phys.* 69: 373, (1997).

[10] D. Boyanovsky, H. J. de Vega, N. G. Sánchez, Phys. Rev. **D 73**, 023008 (2006).

[11] D. Boyanovsky, H. J. de Vega, Lectures at the NATO ASI Chalonge School, 'Current Topics in Astrofundamental Physics', p. 37-57 in the Proceedings edited by N. Sanchez, Kluwer publishers, Series C, vol. 562, 2001, astro-ph/0006446. D. Boyanovsky, D. Cormier, H. J. de Vega, R. Holman et S. Prem Kumar, Phys. Rev. **D 57**, 2166 (1998). F. J. Cao, H. J. de Vega, N. G. Sanchez, Phys. Rev. **D 78**, 083508 (2008).

[12] A. Lasenby, C. Doran, Phys. Rev. D **71**, 063502, (2005) and astro-ph/0411579. A. Lasenby, private communication.

[13] P. R. Anderson, C. Molina-Paris, E. Mottola, Phys. Rev. **D72**, 043515 (2005)

[14] A. Golovnev, V. Mukhanov, V. Vanchurin, JCAP 0806:009 (2008). and 0811:018 (2008). A. Golovnev, V. Vanchurin, Phys. Rev. D79, 103524 (2009). A. Golovnev, Phys. Rev. D 81, 023514 (2010).

[15] D. Boyanovsky, H. J. de Vega, N. G. Sánchez, Nucl. Phys. **B747**, 25 (2006). D. Boyanovsky, H. J. de Vega, N. G. Sánchez, Phys. Rev. **D 72**, 103006 (2005).

[16] H. Leutwyler, Ann. Phys. 235, 165 (1994), hep-ph/9409423. S. Weinberg, hep-ph/9412326 and 'The Quantum Theory of Fields', vol. 2, Cambridge University Press, Cambridge, 2000.

[17] Statistical Physics, vol 9, E M Lifshitz, L P Pitaevsky, Pergamon Press, Oxford 1980, see secs. 142 part I and 45 part II. L. D. Landau, Zh. Eksp. Teor. Fiz., **7**, 19 (1937) and **7**, 545 (1937) and in *Collected Papers of L. D. Landau*, Pergamon Press, Oxford, 1965. V. L. Ginsburg, Zh. Eksp. Teor. Fiz. **15**, 739 and **10**, 107 (1945). V. L. Ginsburg, L. D. Landau, Zh.

Eksp. Teor. Fiz. **20**, 1064 (1950). V. L. Ginsburg, *About Science, Myself and Others*, Part I, Chapters 5-7, IoP, Bristol, 2005.

[18] M. Liguori et al. JCAP **408**, 011 (2004); T. Multamaki, O. Elgaroy, Astronomy and Astrophysics **423**, 811 (2004); C. Gordon, W. Hu, Phys. Rev. **D70**, 083003 (2004); C. R. Contaldi et al., JCAP 0307 (2003) 002; T. R. Jaffe et al. ApJ.**629**, L1 (2005); C. Gordon et al. Phys. Rev. **D72**, 103002 (2005); C-H. Wu et al. JCAP 0702 (2007) 006; L. Campanelli, P. Cea, L. Tedesco, Phys. Rev. Lett. 97, 131302 (2006), Phys. Rev. D76:063007,2007; Y. S. Piao, Phys. Rev. D71, 087301 (2005); M. Kawasaki, F. Takahashi, Phys. Lett. B570, 151 (2003); L. R. Abramo, L. Sodre Jr, C. A. Wuensche, Phys. Rev. D74 (2006) 083515; I-C. Wang, K-W. Ng, Phys. Rev. D 77 (2008) 083501; J. M. Cline et al., JCAP 0309:010, (2003).